Temperature-dependent changes to host-parasite interactions alter the thermal performance of a bacterial host.

Short running title: Host-parasite interactions alter host thermal performance

Author Affiliations

Daniel Padfield[1], Meaghan Castledine[1] & Angus Buckling[1]

[1] College of Life and Environmental Sciences, Environment and Sustainability Institute, University of Exeter, Penryn, Cornwall, TR10 9EZ, U.K.

Corresponding author: Daniel Padfield (d.padfield@exeter.ac.uk)

Author contributions: D.P and A.B conceived the study and designed the experimental work. D.P and M.C conducted the experiments. D.P analysed the data. All authors contributed significantly to the first draft of the manuscript and to revisions.

Data accessibility statement: All data and R code used in the analysis will be made available on GitHub and archived on Zenodo.

Competing interests: There are no competing interests for any of the authors.

Acknowledgements.

We thank 3 anonymous referees for their insightful comments. This work was funded by NERC.

Abstract

Thermal performance curves (TPCs) are used to predict changes in species interactions, and hence, range shifts, disease dynamics and community composition, under forecasted climate change. Species interactions might in turn affect TPCs. Here, we investigate how temperature-dependent changes in a microbial host-parasite interaction (the bacterium *Pseudomonas fluorescens*, and its lytic bacteriophage, SBWΦ2) changes the host TPC and the ecological and evolutionary mechanisms underlying these changes. The bacteriophage had a narrower thermal tolerance for infection, with their critical thermal maximum ~6ºC lower than those at which the bacteria still had high growth. Consequently, in the presence of phage, the host TPC changed, resulting in a lower maximum growth rate. These changes were not just driven by differences in thermal tolerance, with temperature-dependent costs of evolved resistance also playing a major role: the largest cost of resistance occurred at the temperature at which bacteria grew best in the absence of phage. Our work highlights how ecological and evolutionary mechanisms can alter the effect of a parasite on host thermal performance, even over very short timescales.

Introduction

An often overlooked concern surrounding climate change is its impacts on host-parasite interactions [1]. The effect of temperature on species interactions is likely widespread, as temperature influences the physiology, ecology, and evolution of both hosts and parasites [2–5]. However, the sign and strength of the effects of warming on host-parasite interactions may be context dependent, changing with the host, parasite, and environmental conditions in question [6]. One approach to predict the potential impacts of warming on host-parasite interactions has been based around thermal performance curves (TPCs) of, and differences between, key host and parasite traits [2, 6, 7]. For example, it has been argued that as hosts generally have a narrower thermal range and lower thermotolerance than their parasites [8–10], they are more susceptible to disease at temperatures further away from their optimum temperature.

A probable consequence of temperature dependent changes in host-pathogen interactions [11] is a change in the host's TPC in the presence, versus the absence, of the parasite. For example, if the largest impact of the parasite occurs at the host's optimum growth temperature, key traits such as maximum growth rate, optimum temperature of the host could change. In addition to the ecological feedbacks resulting from differences in the thermal performance of host and parasite traits, rapid (co)evolution of resistance and infectivity traits could play a major role in altering TPCs [12, 13]. Crucially, TPCs of hosts and parasites are typically assumed to be fixed across time and in different abiotic and biotic environments [6, 8, 14, 15], but the presence of a predator can alter the TPC of the prey [16] and the prey's evolutionary response to warming [17]. If parasites affect the thermal performance of their host, this may alter some of the predictions of range shifts and disease dynamics expected under climate change.

To date, most experimental and theoretical work on the thermal performance of organisms is done on single species under highly controlled conditions, where naturally occurring parasites, symbionts and microbiota are greatly or completely removed [18–20]. Consequently, it is unknown if parasites alter the TPC of host fitness and influence key species-level traits such as the optimal, T_{opt}, and cardinal (critical thermal maximum, CT_{max}, and minimum, CT_{min}) temperatures of host growth. Understanding these potential impacts is critical to assess the effect of climate change on ecological and evolutionary dynamics of host-parasite pairs, as well as predicting the consequences of novel host-parasite interactions that will occur in a warmer world. Here, we explicitly determine how and why interactions with a parasite affect host thermal performance in arguably the most common host-pathogen interaction on the planet: that between bacteria and their viruses (bacteriophage)[21].

We focus on a well-studied system, the bacterium *Pseudomonas fluorescens* SBW25 and its lytic phage, $SBW\Phi2$. This system has been used extensively for studying host-parasite ecological and evolutionary interactions [22–25]. Over a wide range of temperatures, we measured the replication rate of the phage and the growth rate of the bacteria in the presence and absence of the phage. We utilised the 'traits' that underpin TPCs to compare biologically meaningful parameters [15]. We hypothesised that any large difference in thermal performance of bacteria and phage would change the thermal performance of bacteria in the presence *vs.* the absence of phage. Given the importance of evolution occurring over ecological timescales [26, 27], especially in microbial populations with large population sizes and short generation times, we also investigated evolutionary changes in host populations to determine whether resistance evolution explained any changes in host thermal performance.

Materials and Methods

Measuring bacterial growth in the presence and absence of phage

Isogenic *Pseudomonas fluorescens* SBW25 was cultured overnight (from a frozen stock) at 28 ºC in 6 mL of M9 minimal salts media (M9), supplemented with 5 g of glycerol and 10 g of peptone (50 % concentration of King's medium B) in glass vials at 180 r.p.m. Overnight stocks were then diluted to ~ 50,000 cells per 10 µL (5 x 10^6 cells per mL). Growth curves were measured in 96 well plates, with 180 µL of altered M9 (described above). We inoculated wells with 10 µL of bacteria and either 10 µL of M9 or 10 µL of phage (~50 phage) giving a multiplicity of infection (MOI) of 0.001. We used this low MOI and low starting densities to ensure rapid bacterial growth. Six wells were left free for both bacteria and bacteria plus phage treatments at each temperature as blank controls. We set up 6 replicates of bacteria and bacteria plus phage simultaneously at 8 temperatures (15, 20, 25, 28, 30, 33, 35 and 37 ºC). Each plate was placed in a plastic box with a moist sponge at the bottom to prevent evaporation of media from the wells which may confound measurements of optical density (OD). OD (600 nm wavelength) was measured as a proxy for density of *Pseudomonas fluorescens* using a plate reader (Biotek Instruments Ltd). Readings of OD were taken with the lid off at an average of every 3 hours for up to 75 hours.

Measuring phage replication rate

Replication of the lytic phage SBWΦ2 was measured using methods similar to Knies *et al.* [28, 29], at the same temperatures as the bacterial growth curves, with the addition of 3 additional temperatures (22.5 ºC, 26 ºC and 27 ºC) to better characterise temperatures around the optimum of phage replication. First, isogenic *P. fluorescens* was grown overnight in conditions described above. The bacteria were transferred into fresh media at 28 ºC and allowed to grow for 6 hours while shaking to increase density (~ 10^7 cells). We then added 20 µL of phage (~ 10^6; MOI ~ 0.02, N_0) to each tube (six replicates per temperature). Vials were left static for 4 hours at each temperature, after which phage was extracted using chloroform extraction. 100 µL of

chloroform was added to 900 µL of culture, then vortexed and centrifuged at 10000 g for 5 minutes. The supernatant was removed and placed in fresh Ependorf tubes. Final phage titres, N_4, were measured using plaque assays against the ancestral bacteria at 28 ºC. Phage replication rate, r, was then calculated as $r = \frac{\ln(N_4 - N_0)}{4}$.

Measuring resistance of bacteria

To investigate the mechanism behind any effect of phage on bacterial growth, we measured the resistance of bacteria within a single growth curve. We set up 18 wells of 96 well plates at 8 temperatures that contained ~50,000 cells and ~50 phage (as described above). We then destructively sampled 6 wells at three time points through the growth curve (after 12, 24 and 48 hours). To do this, 20 µL of each well was placed in 180 µL of M9. These were then serially diluted and plated onto KB agar. Twelve colonies from each replicate were taken per time point and grown overnight in 150 µL of altered M9, shaking at 28 ºC. Each clone was then checked for resistance against the ancestral phage using a phage streak assay. Phage streak assays were incubated overnight at 28 ºC.

Measuring the cost of resistance

To determine whether any effect of phage was due to a cost of resistance, we grew 12 replicates of *P. fluorescens* in the presence and absence of phage for 12 hours at 28 ºC. After 12 hours, each population was plated onto KB agar and grown for 2 days at 28 ºC. Three clones were isolated from each replicate and grown for two days in modified M9 media. Each isolate was checked for resistance against the ancestral phage. Growth curves of each clone were done using the methods described above, but inoculate density was ~500,000 cells to reduce the lag time and no phage was added.

Statistical analyses

Calculating exponential growth rate for bacteria

For bacterial growth, we wanted to estimate exponential population growth rate in the presence and absence of phage, and for resistant and susceptible clones. In the presence and absence of phage, prior to model fitting, we removed 3.42% of points (Figures S1-S8) in order to obtain the best estimate of exponential growth at each temperature. The results were qualitatively unchanged by the data cleaning procedure (Figure S9). For a full explanation of the data cleaning procedure please see the supplementary methods section. After this initial data cleaning, we fitted the Gompertz model [30] to measurements of $log_{10}OD_{600}$ through time, t, in hours, using code extracted from the *R* package '*nlsMicrobio*' [31]:

$$log_{10}OD_{600} = log_{10}n_0 + (log_{10}n_{max} - log_{10}n_0) \times e^{(-e^{1+r \times e^1 \times \left(\frac{lag-t}{(log_{10}n_{max} - log_{10}n_0) \times \ln(10)}\right)})} \quad (1)$$

Where $log_{10}n_0$ is the starting density, $log_{10}n_{max}$ is carrying capacity, r is the exponential growth rate (hr^{-1}) and lag is the lag time in hours. Model fitting was done using nonlinear least squares regression using the *R* package '*nls.multstart*' [32]. This method of model fitting involved running up to 500 iterations of the fitting process with start parameters drawn from a uniform distribution and retaining the fit with the lowest Akaike Information Criterion score (AIC). The parameters of the model (r, $log_{10}n_0$, $log_{10}n_{max}$ and lag) can be seen as population-level growth 'traits' which may vary with both temperature and the presence and absence of phage. In this study, r is defined as exponential growth rate of the population and lag is likely determined by the time it takes until growth is detected by the OD reader. Consequently, lag time confounds any actual lag phase with decreases in abundance and slower growth rates that increase the time it takes for abundance to be detected. Other growth models were fitted (e.g. Baranyi, Buchanan; Table S1), but the Gompertz model returned lower AIC scores for the majority of model fits (Figure S10).

For susceptible and resistant clones, we cleaned the data by removing the first measurement (where bubbles due to pipetting could alter the OD reading) and setting time zero to the time at which the first optical density measurement was detected for each clone. We initially used the same modelling approach, but this time the Baranyi model without lag was the model most selected using AIC scores (Figure S11). However, after examining the predictions and residuals of the model fits (Figure S12, Figure S13), we found that exponential growth rate was underestimated at temperatures where bacteria grew best, and at these temperatures there was a significantly greater underestimation of growth rate in susceptible, rather than resistant, bacteria (Figure S14). Consequently, exponential growth rate per clone was calculated here using rolling regression, taking the steepest slope of the linear regression between $lnOD_{600}$ and time in hours in a shifting window of every 4 time points (~7 hours) as the estimate of exponential growth. Average growth rate per replicate was calculated by taking the mean clonal growth rate. After data cleaning and model fitting, every growth curve had estimates of exponential growth rate which were then used to model the thermal performance of bacteria.

Fitting thermal performance curves to phage and bacteria

Thermal performance curves were fitted for phage replication rate and r of bacteria in the presence and absence of phage, and for resistant and susceptible bacterial clones. We used the Sharpe-Schoolfield equation for high-temperature inactivation [33], which extends the original Boltzmann equation to incorporate a decline in growth rate beyond the optimum.

$$b(T) = \frac{b(T_c)e^{E(\frac{1}{kT_c}-\frac{1}{kT})}}{1+e^{E_h(\frac{1}{kT_h}-\frac{1}{kT})}} \quad (2)$$

$b(T)$ is the rate of phage replication or bacterial growth at temperature, T, in Kelvin (K). Instead of the intercept being at 0 K (-273.15 ºC), $b(T_c)$ is the rate at a common temperature,

T_c = 20 ºC (293.15 K)[34]. E (eV) is describes the thermal sensitivity of the biological rate, k is Boltzmann's constant (8.62×10^{-5} eV K^{-1}), E_h (eV) characterises the decline in the rate past the optimum temperature and T_h (K) is the temperature at which half the rate is reduced due to high temperatures. Equation 2 yields an optimum temperature, T_{opt}, (K).

$$T_{opt} = \frac{E_h T_h}{E_h + k T_h ln\left(\frac{E_h}{E} - 1\right)} \quad (3)$$

Maximal growth rate, r_{max}, was calculated by using the estimated model parameters to predict the rate at T_{opt}. As in previous studies [18, 19], these 'traits' were then used to look for differences between (1) bacteria in the presence and absence of phage, and (2) resistant and susceptible bacteria. Similar species-level 'traits' are used in climate change research to explain range shift dynamics [15, 35], but how they are influenced by species interactions remains relatively unknown [16]. As phage replication was negative at high temperatures, an offset was added to the equation to raise all rates above 0 to allow model fitting. This invalidated any interpretation of the thermal sensitivities of phage replication. However, this was already difficult as phage replication is partially determined by bacteria growth rate, which is also temperature dependent and could cause differences in the number of susceptible hosts across temperatures. Consequently, for phage replication we concentrated on the optimum temperature (T_{opt}) and critical thermal maximum (CT_{max}) which is the temperature at which phage replication became negative at high temperatures.

For phage and bacteria, Equation 2 was fitted to the data using non-linear regression in a Bayesian framework using the *R* package '*brms*' [36]. This method allows for prior information on suitable parameter values and the estimation of uncertainty around predictions and parameters, including derived parameters not present in the original model formulation such as T_{opt}, CT_{max} and r_{max}. Different models were fitted for phage replication rate, exponential growth rate of bacteria in the presence and absence of phage, and exponential

214 growth rate of resistant and susceptible bacterial clones. For the analysis including resistant
215 and susceptible clones, a random effect was added to account for the non-independence of
216 measurements of the same clone across temperatures. For bacteria exponential growth rate,
217 phage presence/absence or susceptible/resistance was added as a factor that could alter each
218 parameter of the model. Models were run for 5000 iterations and 3 chains were used with
219 uninformative priors. Model convergence was assessed using posterior predictive checks, Rhat
220 values (all values were 1) and manually checking of chain-mixing. Differences between
221 parameter estimates are described using 95% credible intervals. Credible intervals of
222 predictions and parameters were calculated from the posterior distribution using the *R* package
223 '*tidybayes*' [37]. Non-overlapping 95% credible intervals indicate statistical significance at (at
224 least) the p = 0.05 level.

225 Using predictions from the model for bacterial growth, the relative fitness of bacteria
226 in the presence of phage was estimated across the continuous temperature range (15 – 37 ºC).
227 The difference was calculated as a selection coefficient, where relative fitness at each
228 temperature, $w(T)$, was calculated as:

229 $$w(T) = \frac{r(T)_{bact+phage}}{r(T)_{bact\ alone}} \quad (4)$$

230 where $r(T)_{bact+phage}$ is the growth rate at a given temperature in the presence of phage and
231 $r(T)_{bact\ alone}$is the growth rate in the absence of phage. When the 95% credible intervals of
232 the predictions do not cross 1, it indicates that phage significantly altered bacterial growth rate.
233 When there is overlap with the predictions and 1, it means there is no significant change in
234 relative fitness. An identical statistical approach was taken for analysing the growth rates of
235 susceptible and resistant clones. In this instance, the relative fitness across temperatures, $w(T)$,
236 represented the cost of resistance.

237

238 *Analysing phage resistance assays*

A logistic regression was used to analyse the proportion of resistance through time and across temperatures. A binomial model was fitted to the number of resistant and susceptible individuals per replicate at each temperature and time point using the logit transformation. As there were many populations where all clones were completely susceptible or resistant (resulting in zero and one inflated data), we added one to both the number of resistant and susceptible individuals in each population and used a quasibinomial error structure to control for overdispersion. By adding one to both susceptible and resistant totals, it meant that the model tended to produce slight underestimates for resistance in fully resistant populations, and slight overestimates of resistance in fully susceptible populations, while having little effect on populations with intermediate resistance. This led to the model giving conservative estimates of differences in resistance between temperatures and through time. We fitted a model that combined the number of resistant and susceptible clones in a population as the response variable and included temperature and time (in hours) as discrete predictor variables. Model selection was done through likelihood ratio tests using *F* tests. Pairwise post-hoc comparisons were done on the response scale using the *R* package '*emmeans'* [38]. All analyses were done using the statistical programming language *R* (v3.5.1) [39] and all plots were made using the *R* package '*ggplot2*' [40].

Results

Bacteria and phage had mismatches in their thermal performance

We measured phage replication rate and bacterial growth rate across eight temperature (15 – 37 ºC) to determine whether there were mismatches in the thermal performance of the host and its parasite. To do this, we modelled the thermal performance curve of each rate and used estimated and derived parameters of the model (see Equation 2 in Methods) as traits that we used to compare the thermal responses of bacteria and phage. Phage replication rate increased

to a thermal optimum, T_{opt}, of 27 ºC (95% credible intervals [CI]: 26.5 – 27.5 ºC) before rapidly declining to a negative replication rate by 30 ºC (Fig. 1a). The critical thermal maximum, CT_{max}, of phage replication was 29.2 ºC (95% CI: 29.0 – 29.4 ºC), beyond which phage decreased in abundance over 4 hours (Fig. 1a). This indicated that phage struggled to infect the host at temperatures beyond their T_{opt}, which was similar to previous work that measured the coevolution of this bacteria-phage system across temperatures [25]. The bacteria, *Pseudomonas fluorescens*, had a similar optimum temperature (Fig. 1b [blue]; T_{opt} = 28 ºC; 95% CI: 27.1 – 29.0 ºC), but growth was maintained well beyond T_{opt}, with high growth rates still occurring at 35 ºC (Fig. 1b), > 6 ºC above the CT_{max} of the phage. This could act as a high temperature refuge for the bacteria as phage infection at these temperatures is extremely low. Due to these mismatches in the thermal performance of phage infection and bacterial growth, it was expected that the parasite would alter the thermal performance of its host.

Phage altered the thermal performance of its bacterial host

Due to the thermal mismatches between bacteria and phage, we explored whether phage altered the thermal performance of its host. To do this, we measured the growth rate of bacteria in the presence and absence of the phage and compared key traits that underpinned the thermal performance curve (see Methods). We observed marked differences in the response of bacteria to temperature when in the presence of its phage (Fig. 1b & Table S2). Phage presence changed the optimum temperature of bacterial growth (Fig. 2c), shifting T_{opt} from 28 ºC (95% CI: 27.1 – 29.0 ºC) to 30.6 ºC (95% CI: 29.0 – 32.1 ºC). Moreover, phage presence resulted in a 20.1% (95% CI: 13 - 27.3%) decline in the maximal growth rate, r_{max}, in the presence of phage (Fig. 2d). To better understand the non-linear, temperature dependent effect of phage on bacterial growth, we calculated the relative fitness of bacteria in the presence of phage across temperatures (see Methods; Fig. 2a). The largest impacts of phage on bacterial growth occurred

289 at intermediate temperatures where growth in the absence of phage was highest (Fig. 2a, where
290 relative fitness was <1), whereas no significant change in growth rate was observed at the low
291 and high temperatures measured (credible intervals of predictions overlap 1). The non-linear
292 changes to bacterial growth also resulted in differences in other key traits (Table S2) such as
293 the thermal sensitivity of the rate before (E; Fig. 2b) and after (E_h; Fig. 2e) the optimum
294 temperature.
295
296 *The evolution and cost of resistance was temperature dependent*
297 It is possible that the change in thermal performance of *Pseudomonas fluorescens* could have
298 resulted simply from the mismatches in thermal performances of the host and parasite. Up to
299 T_{opt} of the phage (~27 ºC), phage presence reduced the abundance and thus population growth
300 rate of the bacteria. Consequently, the rapid decline of phage replication at temperatures above
301 30 ºC, while bacteria still had high growth rates, could explain observed shift in the thermal
302 performance of the bacteria. However, bacteria can rapidly evolve resistance to phage within
303 the timescales of our assays, and this has been demonstrated in our host-parasite pair [41, 42].
304 If, as expected, resistance is costly, and resistance does not evolve at temperatures beyond the
305 phage CT_{max}, the effect of phage on the thermal performance of the host may in part be driven
306 by evolutionary change. To investigate this, we measured the resistance of bacteria through a
307 single logistic growth curve at each temperature (Fig. 3). The evolution of phage resistance
308 changed across temperatures and through time, and there was a significant time x temperature
309 interaction (likelihood ratio test comparing models with and without time x temperature
310 interaction: $\Delta d.f.$ = 13, F = 11.56, P < 0.001). There was no measurable resistance in the
311 ancestral bacteria, but after just 12 hours, all populations at 28 ºC (close to T_{opt} of phage
312 replication [~27 ºC]) or lower were close to 100% resistant (Fig. 3a), consistent with a selective
313 sweep in which susceptible cells are lysed and resistant mutants reach fixation. Moreover, after

12 hours, bacterial abundance was much lower than expected at temperatures where phage infection occurred, indicative of a phage epidemic that wiped out susceptible hosts. In contrast, resistance rarely, or never, evolved at temperatures well above those of the critical thermal maximum of phage replication rate (33 ºC and higher, Fig. 3). Where resistance did evolve at these temperatures, it was at very low frequency (1 clone out of 12). We found no bacteria still living at 37 ºC after 48 hours, indicating that although growth occurs at those temperatures, this is quickly proceeded by death.

At temperatures where phage altered the growth rate of bacteria (25, 28 & 30 ºC), we observed significant changes in the proportion of resistance through time (see Table S3 for pairwise differences of resistance through time for each temperature). Resistance evolved and was at high proportions after 12 or 24 hours where populations were still in exponential growth phase. However, after 48 hours, when populations had reached stationary phase at all temperatures apart from 15 and 20 ºC (Figure S15), the proportion of resistance decreased significantly (Fig. 3c). From 24 to 48 hours, 25 ºC resistance fell from 0.89 (95% CI: 0.83 - 0.94) to 0.69 (95% CI: 0.60 – 0.78), at 28 ºC from 0.89 (95% CI: 0.83 - 0.93) to 0.48 (95% CI: 0.40 - 0.57) and at 30 ºC from 0.77 (95% CI 0.68 – 0.83) to 0.17 (95% CI: 0.11 - 0.25). This temporal effect did not occur at low and high temperatures where there was little effect of phage on bacterial growth rate (Fig. 2a & Table S3), suggesting that there was a non-linear cost of resistance across the temperature range.

To confirm whether there was a cost of resistance and if any cost varied with temperature, we isolated clones that were either resistant or susceptible to the phage and measured their thermal performance in the absence of phage. The thermal performance of resistant clones differed from that of susceptible clones (Fig. 4), closely matching the patterns observed when bacteria were grown with phage (Fig. 1b & Fig. 2a). At low and high temperatures, there were no differences in the growth rate of resistant and susceptible clones

(Fig. 4). However, at temperatures where growth of susceptible clones was highest (25 – 30 ºC), there was a cost of resistance (Fig. 4b), resulting in a 13.4% (95% CI: 6.8 - 20.2%) reduction in maximal growth rate. This temperature dependent cost of resistance was qualitatively similar to the effect of phage on bacteria growth, being greatest at intermediate temperatures (Fig. 2a and Fig. 4b).

Discussion

Here, we show that the presence of a parasite can profoundly impact the thermal performance of its host. Notably, phage reduced bacterial growth most at temperatures where the bacteria grew fastest, close to the bacterial r_{max}, while having little or no impact at cold or high temperatures well beyond T_{opt} (Fig. 1 & Fig. 2). This resulted in changes to the thermal performance curve of bacterial growth in the presence of phage (Fig. 2b). These results can be explained by a combination of ecological and evolutionary processes. Ecologically, at temperatures below the critical thermal maxima of the phage, phage presence vastly reduced bacterial abundance (i.e. increased lag time in the logistic growth curve, Figures S1-S4). In contrast, phage could not infect above 30 ºC, but bacteria still had high growth rates. However, rapid evolution also played an important role in altering the thermal performance of *P. fluorescens*. While phage resistance evolved rapidly and was at high levels at all temperatures below the phage CT_{max}, at higher temperatures there was no selection for resistance (Fig. 3). Crucially, there were costs associated with resistance, but these costs changed non-linearly with temperature (Fig. 4). At low temperatures and temperatures far beyond the bacteria T_{opt}, there was no measurable cost of resistance, but significant costs of resistance at intermediate temperatures where bacteria growth was highest (Fig. 4). At some temperatures, susceptible bacteria re-emerged after resistance had evolved (Fig. 3) during stationary phase, which could be a result of nutrient limitation or reduced phage infection of susceptible bacteria in stationary

364 phase [43], both of which would alter the fitness cost of resistance. Overall, these results
365 demonstrate that phage alter the TPC of their host (Fig. 1b) through both ecological (due to
366 differences in thermal tolerance between phage infection and bacterial growth) and
367 evolutionary processes (temperature dependent costs of resistance), resulting in a shift in the
368 TPC for the host in the presence of the phage (Figure S16). It is worth noting that costs of
369 phage resistance were also greatest at the optimum temperature in another well studied
370 bacteria-phage system; *Escherichia coli* and bacteriophage T4 [44, 45].

371 How general are these results likely to be? We suggest that parasites (and symbionts
372 more generally) impacts on host TPCs are likely widespread, because no change in host TPC
373 would occur only when host and parasite traits respond equivalently with temperature. In
374 reality, there are almost certainly mismatches between host and parasite TPCs and differences
375 in local adaptation to prevailing temperatures appears to be the norm [7, 46]. Here, we observed
376 rapid evolutionary interactions between our bacteria-phage pair because of the strong parasite-
377 imposed selection and the large population size and short generation time of *P. fluorescens*
378 (~14 generations after 12 hours at 30 ºC). As this is true of most micro-organisms, we expect
379 that evolutionary mechanisms could frequently drive changes in population-level TPCs,
380 although the selection for resistance is likely to be lower in more heterogeneous environments
381 and with different parasitic lifecycles.

382 Across other host-parasite systems, similar genotype x genotype x environment
383 interactions (G x G x E) occur in different traits, but may be driven more by ecological, rather
384 than evolutionary, processes. For example, in larger, longer-lived hosts, individuals may
385 experience substantial variation in temperature and parasitism over the course of a single
386 generation. In such instances, the individual-level cost of parasitism can still be highest at
387 intermediate temperatures [47] and variation in critical thermal maxima between different host
388 species [8] and thermal mismatches between host and parasite [6] can drive temperature-

389 dependent changes in host susceptibility. Consequently, the effect of parasites on the thermal
390 performance of the host may be widespread across many host-parasite systems, driven by
391 ecological or rapid evolutionary processes depending on host lifespan and magnitude of
392 parasite-imposed selection.

393 However, as with the effect of changing temperature on disease severity, precisely how
394 TPCs will change will be context dependent, changing with, amongst other factors, the host-
395 parasite pair and the biological traits measured. For example, phage replication across
396 temperature depends on the thermal sensitivity of multiple processes such as latency period,
397 burst size, and thermal stability [48], such that the limiting factor for phage replication may
398 also differ across temperature. Moreover, the effect of any of these phage traits in isolation
399 may result in a different impact on the host TPC. Marine phage are generally more thermally
400 stable than their hosts [9], but, as shown here, it that does not mean that the phage can infect at
401 all temperatures [49]. Across ectotherms, thermal breadth across multiple traits is generally
402 wider in smaller organisms [10], but whether this impacts host or parasite TPCs (parasites are
403 generally smaller than their host) in the presence of each other remains to be seen.

404 In conclusion, our study demonstrated that host-parasite interactions change in non-
405 linear ways with temperature (G x G x E interaction), and this had a significant impact on the
406 thermal performance of the host. By measuring the thermal performance of the host and the
407 parasite simultaneously, and also examining the evolution and cost of resistance, we identified
408 the mechanisms through which phage altered the thermal performance of the host. Our results
409 highlight that TPCs measured under axenic conditions should be interpreted with caution;
410 measuring TPCs in the absence of their parasites (and other associated microbiota) may not be
411 reflective of the host's TPC in nature where such interactions are ubiquitous. Future work
412 should investigate the longer term evolutionary and coevolutionary consequences of climate
413 warming [13] and in a broader, more realistic ecological context, to determine how this impacts

414 host-parasite interactions. In an era of human-induced climate change, it is more important than
415 ever to gain a deeper understanding of how evolutionary and ecological processes can
416 indirectly impact thermal performance and how host-parasite interactions will change with
417 temperature.
418

References

1. Harvell CD, Mitchell CE, Ward JR, Altizer S, Dobson AP, Ostfeld RS, et al. Climate warming and disease risks for terrestrial and marine biota. *Science* 2002; **296**: 2158–2162.
2. Demory D, Arsenieff L, Simon N, Six C, Rigaut-Jalabert F, Marie D, et al. Temperature is a key factor in Micromonas–virus interactions. *The ISME journal* 2017; **11**: 601.
3. Paull SH, LaFonte BE, Johnson PT. Temperature-driven shifts in a host-parasite interaction drive nonlinear changes in disease risk. *Global Change Biology* 2012; **18**: 3558–3567.
4. Paull SH, Raffel TR, LaFonte BE, Johnson PT. How temperature shifts affect parasite production: testing the roles of thermal stress and acclimation. *Functional Ecology* 2015; **29**: 941–950.
5. Molnár PK, Kutz SJ, Hoar BM, Dobson AP. Metabolic approaches to understanding climate change impacts on seasonal host-macroparasite dynamics. *Ecology Letters* 2013; **16**: 9–21.
6. Cohen JM, Venesky MD, Sauer EL, Civitello DJ, McMahon TA, Roznik EA, et al. The thermal mismatch hypothesis explains host susceptibility to an emerging infectious disease. *Ecology letters* 2017; **20**: 184–193.
7. Gehman A-LM, Hall RJ, Byers JE. Host and parasite thermal ecology jointly determine the effect of climate warming on epidemic dynamics. *Proceedings of the National Academy of Sciences* 2018; 201705067.
8. Nowakowski AJ, Whitfield SM, Eskew EA, Thompson ME, Rose JP, Caraballo BL, et al. Infection risk decreases with increasing mismatch in host and pathogen environmental tolerances. *Ecology letters* 2016; **19**: 1051–1061.

9. Mojica KD, Brussaard CP. Factors affecting virus dynamics and microbial host–virus interactions in marine environments. *FEMS microbiology ecology* 2014; **89**: 495–515.
10. Rohr JR, Civitello DJ, Cohen JM, Roznik EA, Sinervo B, Dell AI. The complex drivers of thermal acclimation and breadth in ectotherms. *Ecology letters* 2018; **21**: 1425–1439.
11. Thomas MB, Blanford S. Thermal biology in insect-parasite interactions. *Trends in Ecology & Evolution* 2003; **18**: 344–350.
12. Tseng M, Bernhardt JR, Chila AE. Species interactions mediate thermal evolution. *Evolutionary Applications* .
13. Gorter FA, Scanlan PD, Buckling A. Adaptation to abiotic conditions drives local adaptation in bacteria and viruses coevolving in heterogeneous environments. *Biology letters* 2016; **12**: 20150879.
14. Sinclair BJ, Marshall KE, Sewell MA, Levesque DL, Willett CS, Slotsbo S, et al. Can we predict ectotherm responses to climate change using thermal performance curves and body temperatures? *Ecology Letters* 2016; **19**: 1372–1385.
15. Sunday JM, Bates AE, Dulvy NK. Thermal tolerance and the global redistribution of animals. *Nature Climate Change* 2012; **2**: 686–690.
16. Luhring TM, DeLong JP. Predation changes the shape of thermal performance curves for population growth rate. *Current zoology* 2016; **62**: 501–505.
17. Tseng M, O'Connor MI. Predators modify the evolutionary response of prey to temperature change. *Biology letters* 2015; **11**: 20150798.
18. Padfield D, Yvon-Durocher G, Buckling A, Jennings S, Yvon-Durocher G. Rapid evolution of metabolic traits explains thermal adaptation in phytoplankton. *Ecology Letters* 2016; **19**: 133–142.

19. Schaum C-E, Barton S, Bestion E, Buckling A, Garcia-Carreras B, Lopez P, et al. Adaptation of phytoplankton to a decade of experimental warming linked to increased photosynthesis. *Nature Ecology & Evolution* 2017; **1**: 0094.
20. Angilletta Jr MJ. Thermal adaptation: a theoretical and empirical synthesis. 2009. Oxford University Press.
21. Clokie MR, Millard AD, Letarov AV, Heaphy S. Phages in nature. *Bacteriophage* 2011; **1**: 31–45.
22. Lopez-Pascua, L.D.C, Buckling A. Increasing productivity accelerates host–parasite coevolution. *Journal of evolutionary biology* 2008; **21**: 853–860.
23. Buckling A, Rainey PB. Antagonistic coevolution between a bacterium and a bacteriophage. *Proceedings of the Royal Society of London B: Biological Sciences* 2002; **269**: 931–936.
24. Gómez P, Buckling A. Bacteria-phage antagonistic coevolution in soil. *Science* 2011; **332**: 106–109.
25. Zhang Q-G, Buckling A. Antagonistic coevolution limits population persistence of a virus in a thermally deteriorating environment. *Ecology letters* 2011; **14**: 282–288.
26. Ellner SP, Geber MA, Hairston Jr NG. Does rapid evolution matter? Measuring the rate of contemporary evolution and its impacts on ecological dynamics. *Ecology letters* 2011; **14**: 603–614.
27. Hairston Jr NG, Ellner SP, Geber MA, Yoshida T, Fox JA. Rapid evolution and the convergence of ecological and evolutionary time. *Ecology letters* 2005; **8**: 1114–1127.
28. Knies JL, Izem R, Supler KL, Kingsolver JG, Burch CL. The genetic basis of thermal reaction norm evolution in lab and natural phage populations. *PLoS biology* 2006; **4**: e201.

29. Knies JL, Kingsolver JG, Burch CL. Hotter is better and broader: thermal sensitivity of fitness in a population of bacteriophages. *The American Naturalist* 2009; **173**: 419–430.
30. Gompertz B. On the nature of the function expressive of the law of human mortality, and on a new mode of determining the value of life contingencies. *Philosophical Transactions of the Royal Society of London B: Biological Sciences* 1825; **115**: 513–583.
31. Baty F, Delignette-Muller ML. nlsMicrobio: Nonlinear regression in predictive microbiology. R package version 3.2. 2. 2016.
32. Padfield D, Matheson G. nls.multstart: Robust Non-Linear Regression using AIC Scores. R package version 1.0.0. 2018.
33. Schoolfield RM, Sharpe PJH, Magnuson CE. Non-linear regression of biological temperature-dependent rate models based on absolute reaction-rate theory. *Journal of theoretical biology* 1981; **88**: 719–731.
34. Padfield D, Buckling A, Warfield R, Lowe C, Yvon-Durocher G. Linking phytoplankton community metabolism to the individual size distribution. *Ecology Letters* 2018.
35. Sunday JM, Pecl GT, Frusher S, Hobday AJ, Hill N, Holbrook NJ, et al. Species traits and climate velocity explain geographic range shifts in an ocean-warming hotspot. *Ecology letters* 2015; **18**: 944–953.
36. Bürkner P-C. brms: An R package for Bayesian multilevel models using Stan. *Journal of Statistical Software* 2017; **80**: 1–28.
37. Kay M. tidybayes: Tidy Data and Geoms for Bayesian Models. 2018.
38. Lenth R. Emmeans: Estimated marginal means, aka least-squares means. *R Package Version* 2018; **1**.
39. Team RC. R: A language and environment for statistical computing. 2013.
40. Wickham H. ggplot2: elegant graphics for data analysis. 2016. Springer.

41. Buckling A, Rainey PB. The role of parasites in sympatric and allopatric host diversification. *Nature* 2002; **420**: 496.
42. Lenski RE, Levin BR. Constraints on the coevolution of bacteria and virulent phage: a model, some experiments, and predictions for natural communities. *The American Naturalist* 1985; **125**: 585–602.
43. Bryan D, El-Shibiny A, Hobbs Z, Porter J, Kutter EM. Bacteriophage T4 infection of stationary phase E. coli: Life after log from a phage perspective. *Frontiers in microbiology* 2016; **7**: 1391.
44. Quance MA, Travisano M. Effects of temperature on the fitness cost of resistance to bacteriophage T4 in Escherichia coli. *Evolution: International Journal of Organic Evolution* 2009; **63**: 1406–1416.
45. Cooper VS, Bennett AF, Lenski RE. Evolution of thermal dependence of growth rate of Escherichia coli populations during 20,000 generations in a constant environment. *Evolution* 2001; **55**: 889–896.
46. Dell AI, Pawar S, Savage VM. Systematic variation in the temperature dependence of physiological and ecological traits. *Proceedings of the National Academy of Sciences* 2011; **108**: 10591–10596.
47. Kirk D, Jones N, Peacock S, Phillips J, Molnár PK, Krkošek M, et al. Empirical evidence that metabolic theory describes the temperature dependency of within-host parasite dynamics. *PLoS biology* 2018; **16**: e2004608.
48. Sillankorva S, Oliveira R, Vieira MJ, Sutherland I, Azeredo J. Pseudomonas fluorescens infection by bacteriophage ΦS1: the influence of temperature, host growth phase and media. *FEMS microbiology letters* 2004; **241**: 13–20.

536 49. Delisle AL, Levin RE. Characteristics of three phages infectious for psychrophilic fishery
537 isolates ofPseudomonas putrefaciens. *Antonie van Leeuwenhoek* 1972; **38**: 1–8.
538
539

Figures

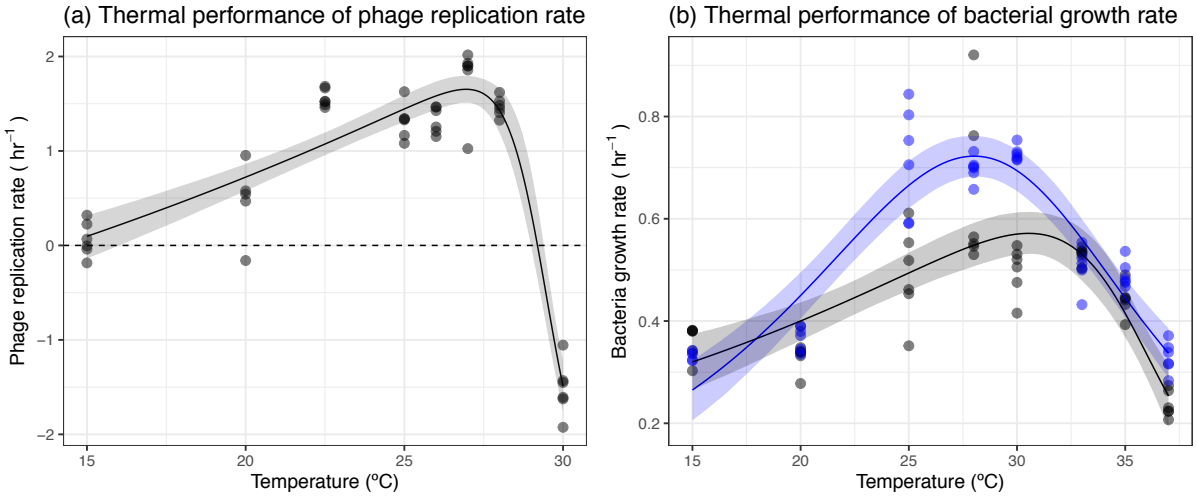

Figure 1. Thermal performance of phage and bacteria. (a) Phage replication increases with temperature up to an optimum of before declining rapidly to a negative replication rate at 30 ºC. (b) Bacteria growth shows unimodal responses to temperature in the presence (black) and absence of phage (blue). However, phage changed the shape of the thermal response. Points represent an independent replicate at each temperature. Solid lines represent the mean prediction and shaded bands represent the 95% credible interval of predictions. In (a) the dashed line represents 0 growth, below which phage abundance decreased. In (b), the dashed line represents the CT_{max} of the phage, beyond which phage abundance decreased.

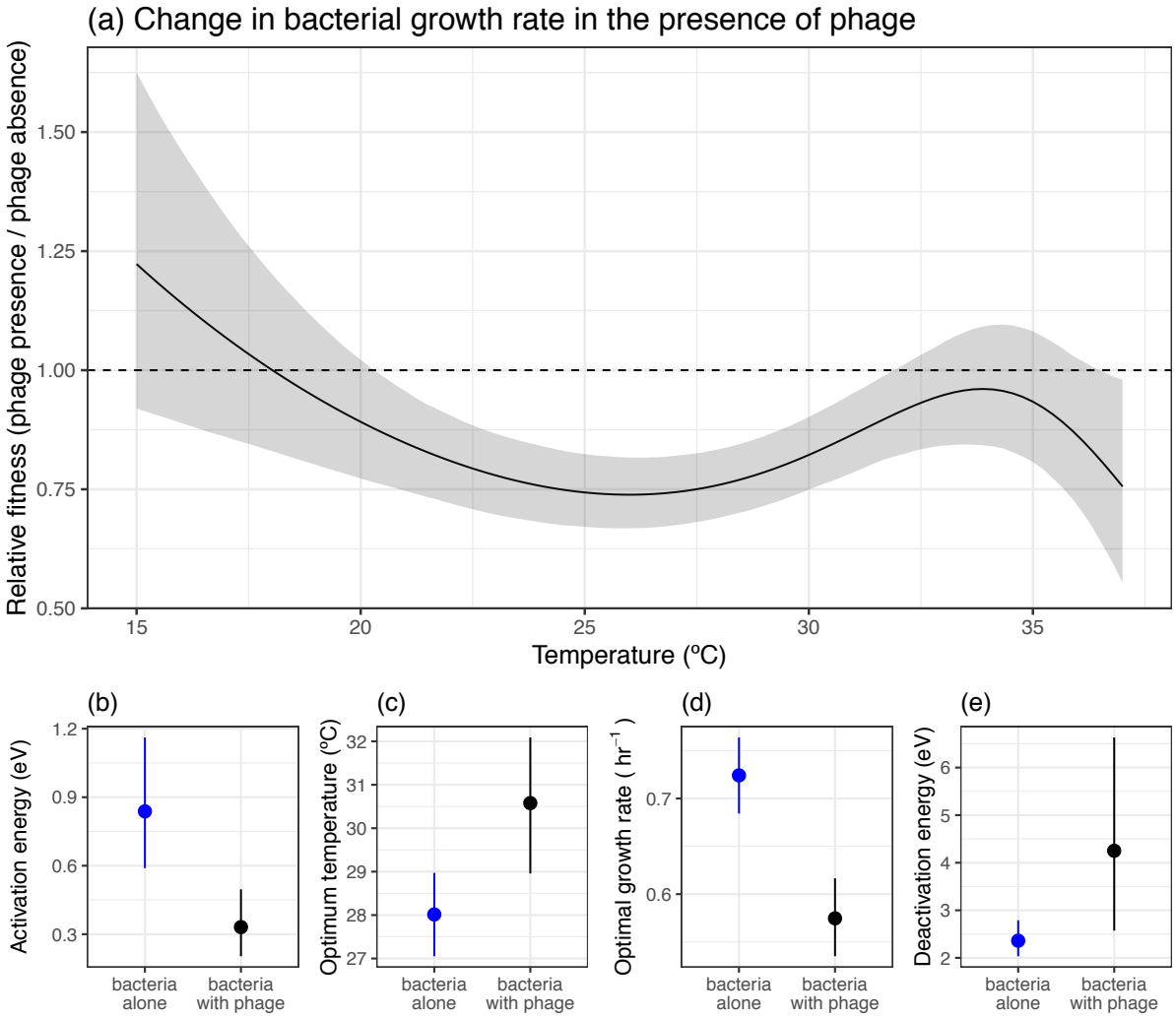

Figure 2. Effect of phage on the thermal performance of bacteria. (a) Phage altered the growth rate of bacteria (calculated as relative fitness) in a non-linear fashion with increasing temperatures. (b-e) The effect of phage on key thermal performance traits. Phage altered the (b) activation energy, (c) optimum temperature, (d) optimal growth rate and (e) deactivation energy. In (a) the solid line represents the mean prediction and shaded band represents the 95% credible interval of predictions. The dashed line at y = 1 would indicate that phage do not alter growth rate. Below 1, phage reduces the growth rate of the bacteria. In (b-e) points and lines represent the mean and 95% credible intervals of the estimated parameters.

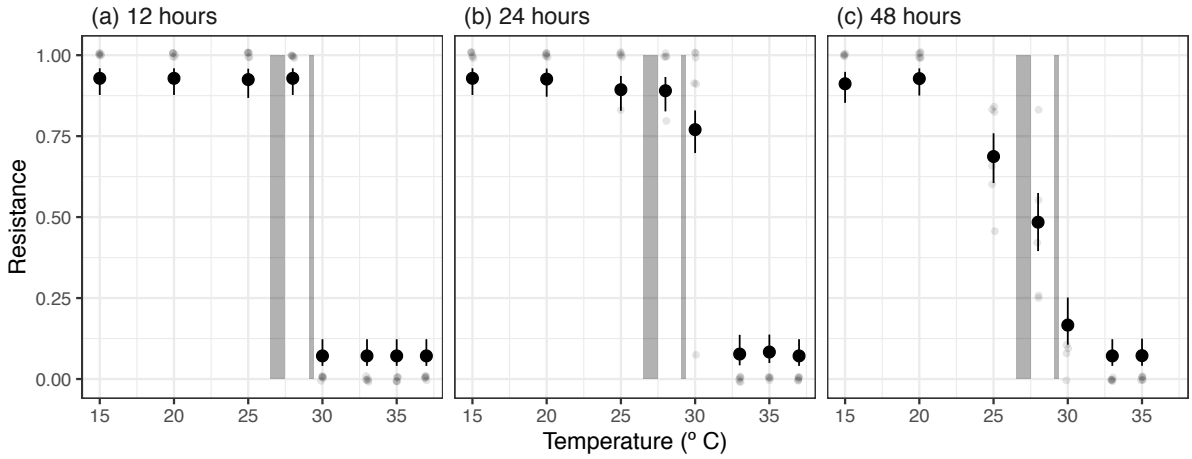

Figure 3. Levels of resistance of *Pseudomonas fluorescens* to phage through time and across temperatures. After 12 hours, populations are completely resistant at temperatures of 28 ºC or lower. After 24 hours, most bacteria populations at 30 ºC, close to the estimated critical thermal maxima (CT_{max}) of the phage, have evolved resistance, but populations beyond the CT_{max} of phage infection remain susceptible. After 48 hours, at temperatures where phage impact bacterial growth, intermediate levels of resistance are observed. Small points represent the observed level of resistance for a population. Large points represent the predicted levels of resistance (of transformed data [see Methods]) from a binomial regression with 95% confidence intervals. Shaded regions represent the upper and lower confidence intervals of the optimum temperature and critical thermal maxima of the phage.

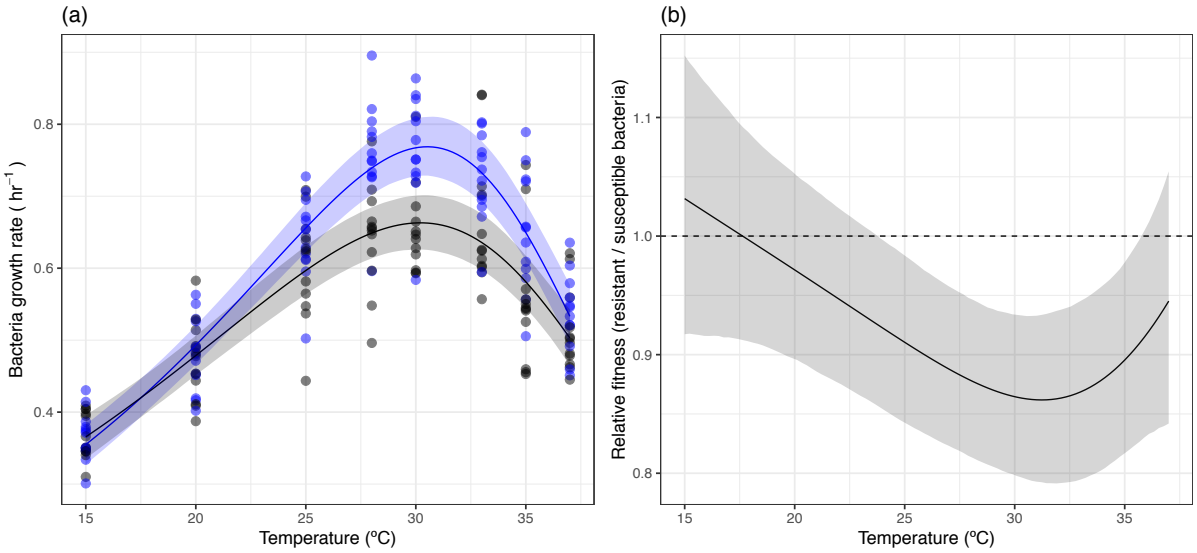

573

574 **Figure 4. Temperature dependent cost of resistance in *Pseudomonas fluorescens* in the**
575 **absence of phage.** (a) The thermal performance of susceptible (blue) and resistant (black)
576 clones. Resistant clones have a lower maximum growth rate. (b) The derived selection
577 coefficient of resistance across temperatures. The cost of resistance changes across
578 temperatures, being greatest at 30 ºC and other temperatures where growth in the absence of
579 phage is high. In (a) points represent individual clones, solid lines represent the mean prediction
580 and shaded bands represent the 95% credible interval of predictions. In (b) the dashed line at y
581 = 1 would indicate that phage do not alter growth rate. Below 1, phage reduces the growth rate
582 of the bacteria.

583

584

Supplementary Information for: Temperature-dependent changes to host-parasite interactions alter the thermal performance of a bacterial host.

Author Affiliations

Daniel Padfield[1], Meaghan Castledine[1] & Angus Buckling[1]

[1] College of Life and Environmental Sciences, Environment and Sustainability Institute, University of Exeter, Penryn, Cornwall, TR10 9EZ, U.K.

Corresponding author: Daniel Padfield (d.padfield@exeter.ac.uk)

Author contributions: D.P and A.B conceived the study and designed the experimental work. D.P and M.C conducted the experiments. D.P analysed the data. All authors contributed significantly to the first draft of the manuscript and to revisions.

Data accessibility statement: All data and R code used in the analysis will be made available on GitHub and archived on Zenodo.

Supplementary methods

Data cleaning and model selection process

When processing the data on bacterial growth from the optical density reader, we first corrected the raw OD_{600} by the blank control (OD_{600} corrected = OD_{600} observed – OD_{600} blank). As the inoculum of the bacteria was too small to be accurately measured by the OD reader, if OD_{600} corrected was less than the smallest value the OD reader could measure (0.001), the value was replaced with 0.001. This meant that the estimate of lag time estimates the time at which the bacteria could first be measured by the OD reader, but does not impact any of the estimates of exponential growth.

In the presence of phage, to ensure that the best possible estimate of exponential growth was obtained, we implemented data cleaning after visualising the data. This is because during the bacterial growth curve, phage infections occur which result in decreases in abundance that are not expected based on the shape of the logistic growth curve. Moreover, where in the logistic growth curve these abundance changes due to phage infection occur alters the effect on the logistic growth curve. If lysis of host cells occurred in the lag phase (as determined by the model; Figure S1-S4), there is little to no impact of these changes in abundance on the model fit. However, at 30 ºC (Figure S5), the lysis of host cells occurred in mid-log growth phase and consequently drastically changes the estimate of exponential growth obtained from the model (Figure S5; red line). Consequently, we removed the points that we were certain were a result of phage infection (Figure S1-S8; red points) and then modelled the data. This resulted in the removal of 3.42 % of all points. Reassuringly, if the analysis of TPCs was run on the estimates of exponential growth of the raw data, similar results were obtained (Figure S17), with the biggest cost difference in fitness occurring at intermediate temperatures.

For susceptible and resistant clones, the higher inoculum (ten-fold higher), and a lack of phage, resulted in an alternative data cleaning procedure being implemented. The higher inoculum resulted in fewer readings being initially beyond the range of the OD reader, and therefore a model without a lag time was favoured in most cases. Instead, we simply removed the first measurement (which was prone to error due to the bubbles present after pipetting the inoculum) and set time zero to the time at which the first optical density measurement was detected for each clone.

Table S1. Logistical growth equations used in the modelling of bacterial growth in the presence and absence of phage.

Model	Equation
Gompertz	$log_{10}OD_{600} = log_{10}n_0 + (log_{10}n_{max} - log_{10}n_0) \times e^{(-e^{1+r \times e^1 \times \left(\frac{lag-t}{(log_{10}n_{max} - log_{10}n_0) \times \ln(10)}\right)})}$
Baranyi	$log_{10}OD_{600} = log_{10}n_{max} + log_{10}\left(\frac{-1+e^{r \times lag}+e^{r \times t}}{e^{r \times t}-1+e^{r \times lag} \times 10^{(log_{10}n_{max} - log_{10}n_0)}}\right)$
Baranyi without lag	$log_{10}OD_{600} = log_{10}n_{max} - log_{10}\left(1 + (10^{(log_{10}n_{max} - log_{10}n_0)} - 1) \times e^{-r \times t}\right)$
Buchanan	$log_{10}OD_{600} = log_{10}n_0$ for when $t \leq lag$ $log_{10}OD_{600} = log_{10}n_0 + r(t - lag)$ for when $lag \leq t \leq t_s$ $log_{10}OD_{600} = log_{10}n_{max}$ for when $t \geq t_s$
Buchanan without lag	$log_{10}OD_{600} = log_{10}n_0 + r(t - lag)$ for when $t \leq t_s$ $log_{10}OD_{600} = log_{10}n_{max}$ for when $t \geq t_s$

Where $log_{10}OD_{600}$ is the log10 of the absorbance measurement, $log_{10}n_0$ is the starting density, $log_{10}n_{max}$ is carrying capacity, r is the exponential growth rate (hr^{-1}), lag is the lag time in hours and t_s is the time to stationary phase in hours. Model equations were copied from the R package '*nlsMicrobio*'. Code for fitting each equation and comparing AIC scores can be found on the GitHub repository for this manuscript.

Table S2. Point estimates and 95% credible intervals (as determined using Bayesian methods) for fitted and derived metabolic traits.

Rate	Parameter	Mean	2.5%	97.5%
phage replication	CT_{max} (ºC)	29.2	29	29.4
	T_{opt} (ºC)	27.0	26.5	27.5
bacteria growth without phage	E (eV)	0.84	0.59	1.16
	E_h (eV)	2.36	2.03	2.79
	T_{opt} (ºC)	28.0	27.1	29.0
	r_{max} (hr^{-1})	0.72	0.68	0.76
bacteria growth with phage	E (eV)	0.33	0.20	0.50
	E_h (eV)	4.25	2.57	6.63
	T_{opt} (ºC)	30.6	29.0	32.1
	r_{max} (hr^{-1})	0.57	0.54	0.62
bacteria growth of susceptible clones	E (eV)	0.49	0.42	0.57
	E_h (eV)	2.32	1.95	2.77
	T_{opt} (ºC)	30.5	30.0	31.0
	r_{max} (hr^{-1})	0.77	0.73	0.81
bacteria growth of resistant clones	E (eV)	0.42	0.33	0.56
	E_h (eV)	1.95	1.47	2.57
	T_{opt} (ºC)	30.2	29.2	31.0
	r_{max} (hr^{-1})	0.66	0.63	0.70
bacteria growth	% change in r_{max} due to presence of phage	-20.6	-13.1	-27.3
	% change in r_{max} due to phage resistance	-13.6	-6.8	-20.2

Parameters include CT_{max}, the critical thermal maximum, T_{opt}, the optimum temperature, E, the activation energy, E_h, the deactivation energy, r_{max}, the maximum growth rate and the % change in maximum growth rate due to phage presence and due to phage resistance. Not all parameters are shown for each rate because they were either outside the range of the data collected or were not biologically meaningful for the data collected.

Table S3. Results of multiple pairwise comparisons between resistance through time at each temperature.

Temperature	Contrast	Odds ratio	SE	z ratio	p value
15	12 hours vs. 24 hours	1	0.43	0	1
	12 hours vs. 48 hours	1.26	0.54	0.54	0.85
	24 hours vs. 48 hours	1.26	0.54	0.54	0.85
20	12 hours vs. 24 hours	1.04	0.45	0.08	0.99
	12 hours vs. 48 hours	1.01	0.44	0.03	0.99
	24 hours vs. 48 hours	0.98	0.43	-0.05	0.99
25	12 hours vs. 24 hours	1.16	0.62	0.89	0.65
	12 hours vs. 48 hours	5.61	2.05	4.71	<0.001
	24 hours vs. 48 hours	3.85	1.29	4.02	<0.001
28	12 hours vs. 24 hours	1.62	0.66	1.17	0.47
	12 hours vs. 48 hours	13.9	4.96	7.36	<0.001
	24 hours vs. 48 hours	8.60	2.81	6.59	<0.001
30	12 hours vs. 24 hours	0.02	0.01	-10.46	<0.001
	12 hours vs. 48 hours	0.37	0.16	-2.35	0.049
	24 hours vs. 48 hours	16.8	5.48	8.68	<0.001
33	12 hours vs. 24 hours	0.92	0.41	-0.19	0.98
	12 hours vs. 48 hours	1	0.43	0	1
	24 hours vs. 48 hours	1.1	0.49	0.194	0.98
35	12 hours vs. 24 hours	0.85	0.35	-0.40	0.92
	12 hours vs. 48 hours	0.99	0.43	-0.03	0.99
	24 hours vs. 48 hours	1.12	0.49	0.37	0.93
37	12 hours vs. 24 hours	1	0.433	0	1
	12 hours vs. 48 hours	-	-	-	-
	24 hours vs. 48 hours	-	-	-	-

At temperatures where growth was highest, resistance changed significantly through time. P values were adjusted using the Tukey method for comparing a family of 3 estimates and tests were performed on the log odds ratio scale. An odds ratio of 1 would indicate that resistance was the same in both groups, with a higher odds ratio indicating that resistance was higher in the first group, and a lower odds ratio would indicate that resistance was higher in the second group.

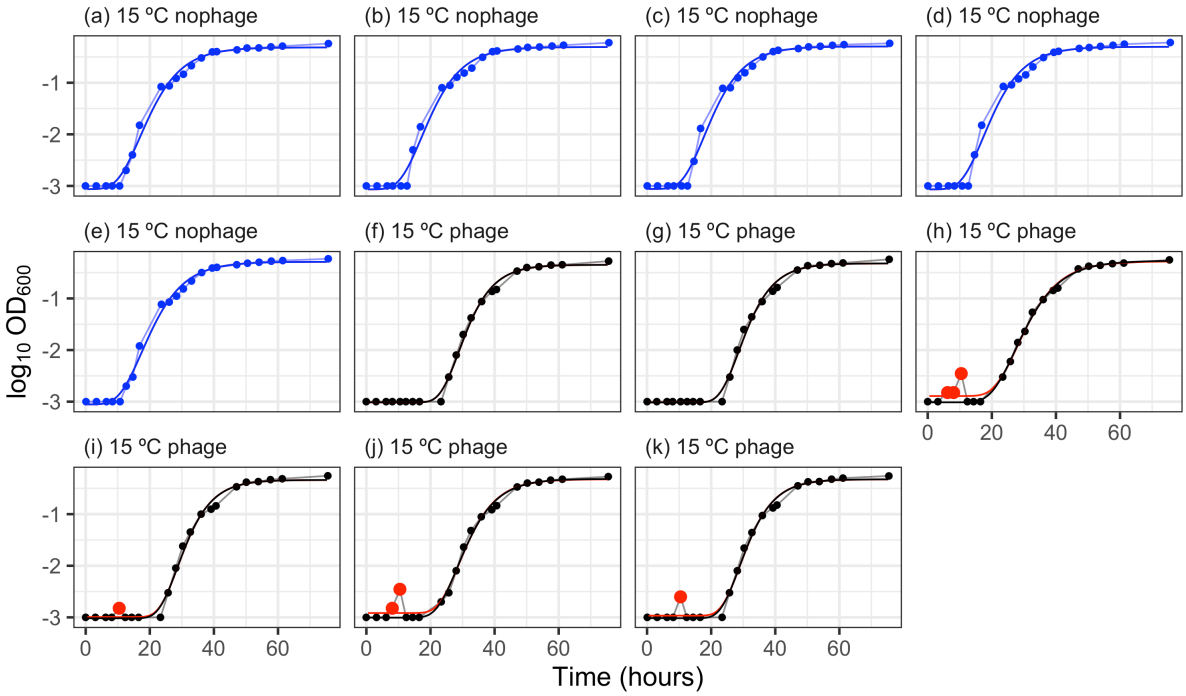

Figure S1. Effect of data cleaning on logistic growth curves for bacterial growth in the presence (black) and absence (blue) of phage at 15 ºC. The Gompertz model for logistic growth was fitted to each independent replicate and the exponential growth parameter was extracted for use in the thermal performance curves. Points that were removed in the final dataset and predictions of the model using the raw dataset are shown in red. A lack of red indicates no points were removed and predictions are equal between the two datasets. Points represent individual measurements and lines represent predictions of the best fitting model for each replicate at each temperature.

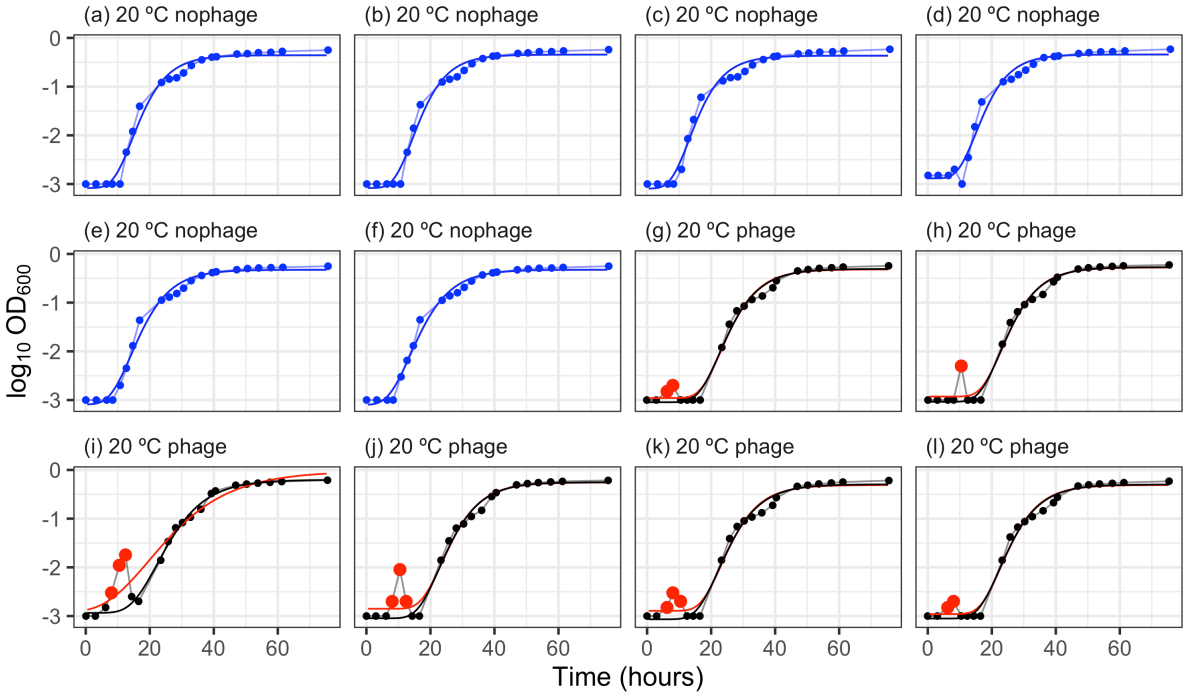

Figure S2. Effect of data cleaning on logistic growth curves for bacterial growth in the presence (black) and absence (blue) of phage at 20 °C. The Gompertz model for logistic growth was fitted to each independent replicate and the exponential growth parameter was extracted for use in the thermal performance curves. Points that were removed in the final dataset and predictions of the model using the raw dataset are shown in red. A lack of red indicates no points were removed and predictions are equal between the two datasets. Points represent individual measurements and lines represent predictions of the best fitting model for each replicate at each temperature.

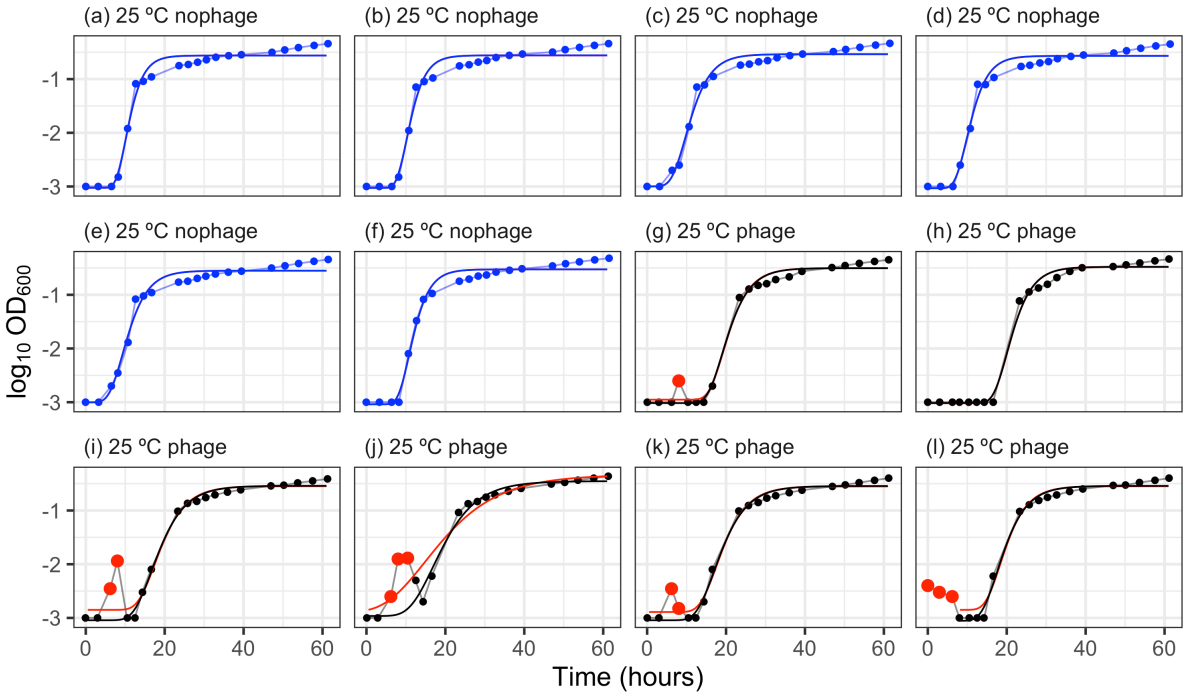

Figure S3. Effect of data cleaning on logistic growth curves for bacterial growth in the presence (black) and absence (blue) of phage at 25 °C. The Gompertz model for logistic growth was fitted to each independent replicate and the exponential growth parameter was extracted for use in the thermal performance curves. Points that were removed in the final dataset and predictions of the model using the raw dataset are shown in red. A lack of red indicates no points were removed and predictions are equal between the two datasets. Points represent individual measurements and lines represent predictions of the best fitting model for each replicate at each temperature.

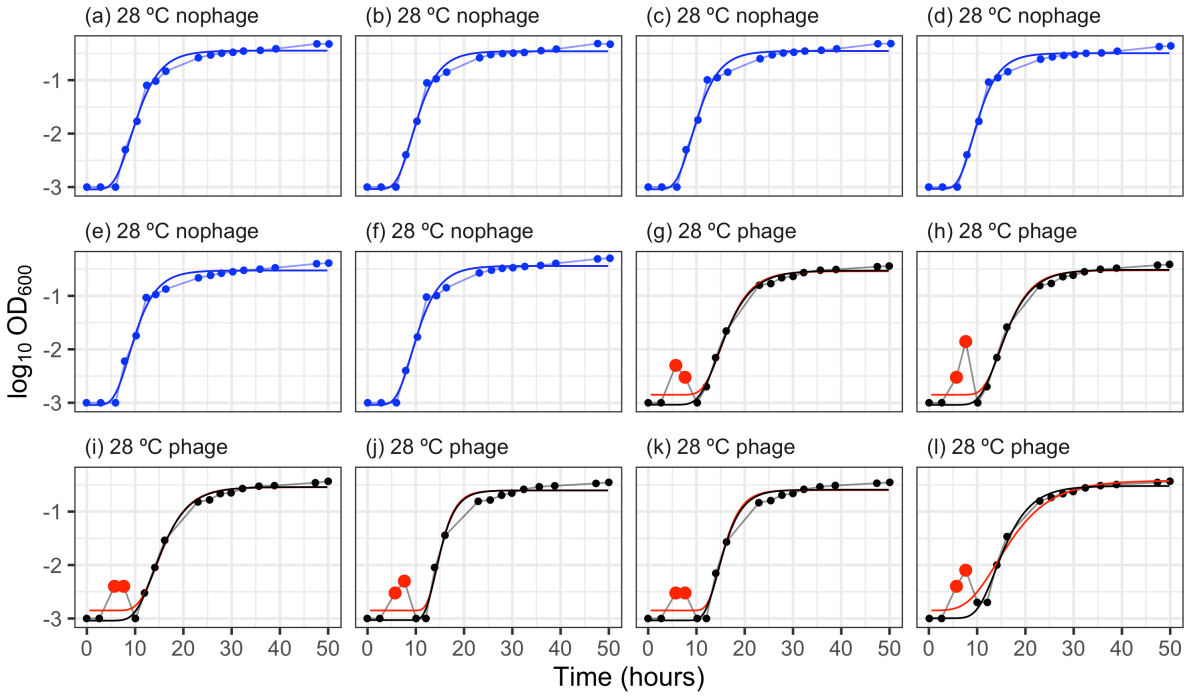

Figure S4. Effect of data cleaning on logistic growth curves for bacterial growth in the presence (black) and absence (blue) of phage at 28 °C. The Gompertz model for logistic growth was fitted to each independent replicate and the exponential growth parameter was extracted for use in the thermal performance curves. Points that were removed in the final dataset and predictions of the model using the raw dataset are shown in red. A lack of red indicates no points were removed and predictions are equal between the two datasets. Points represent individual measurements and lines represent predictions of the best fitting model for each replicate at each temperature.

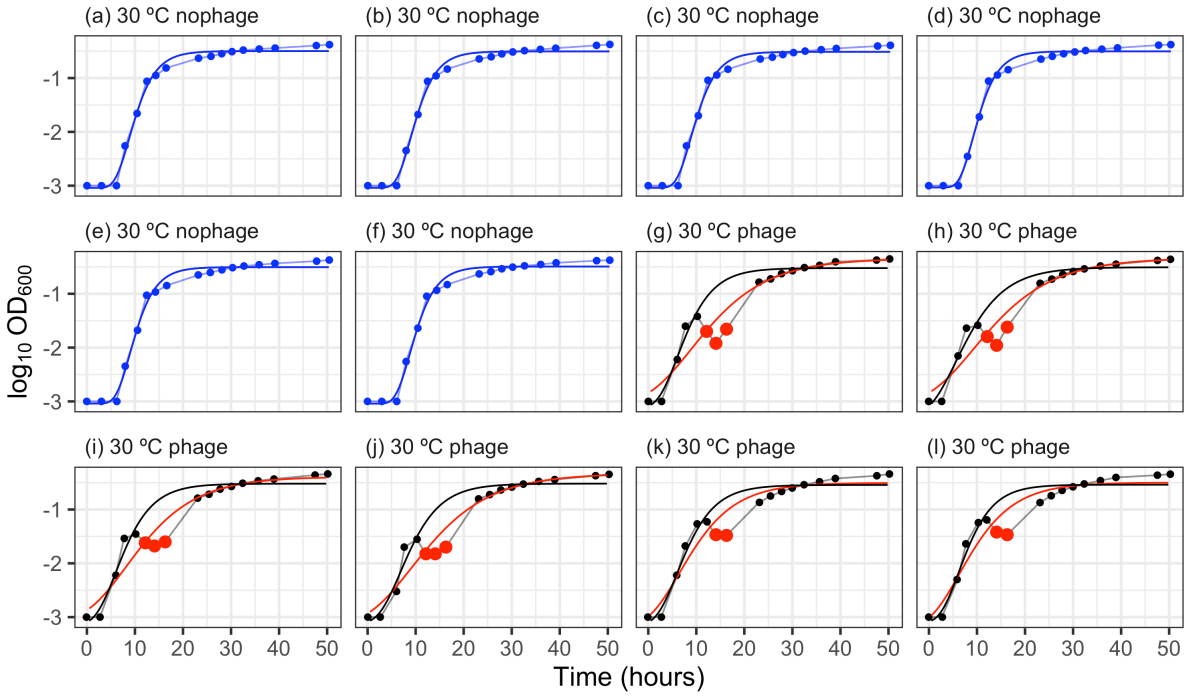

Figure S5. Effect of data cleaning on logistic growth curves for bacterial growth in the presence (black) and absence (blue) of phage at 30 °C. The Gompertz model for logistic growth was fitted to each independent replicate and the exponential growth parameter was extracted for use in the thermal performance curves. Points that were removed in the final dataset and predictions of the model using the raw dataset are shown in red. A lack of red indicates no points were removed and predictions are equal between the two datasets. Points represent individual measurements and lines represent predictions of the best fitting model for each replicate at each temperature.

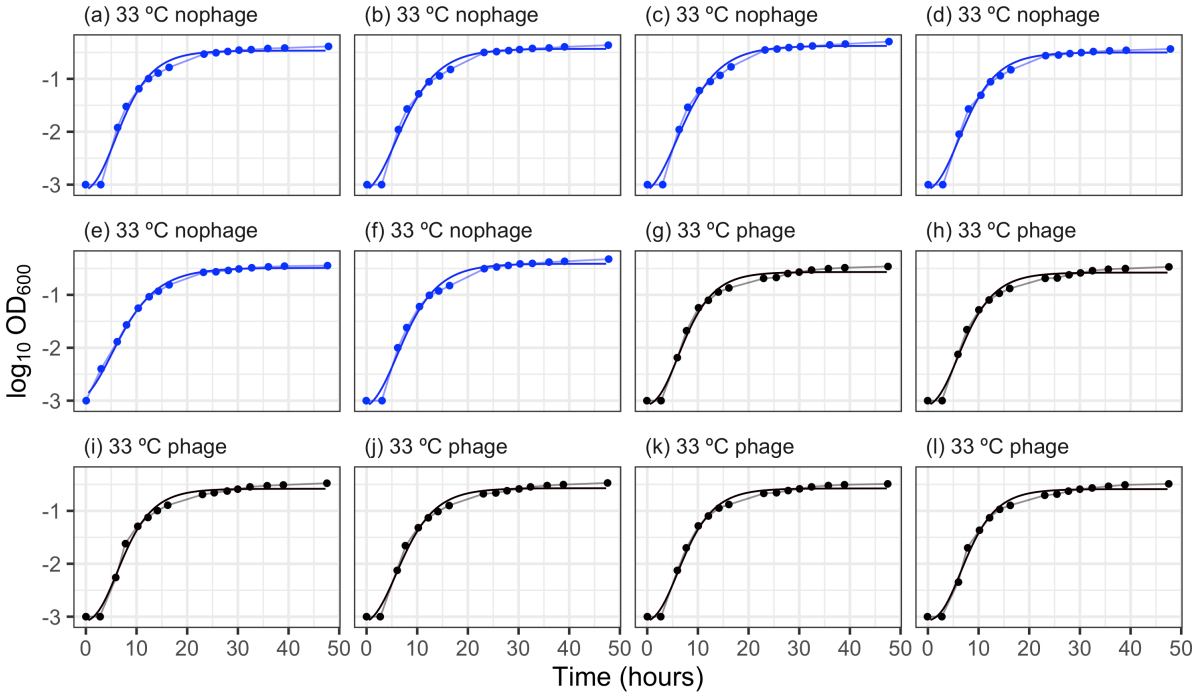

Figure S6. Effect of data cleaning on logistic growth curves for bacterial growth in the presence (black) and absence (blue) of phage at 33 °C. The Gompertz model for logistic growth was fitted to each independent replicate and the exponential growth parameter was extracted for use in the thermal performance curves. Points that were removed in the final dataset and predictions of the model using the raw dataset are shown in red. A lack of red indicates no points were removed and predictions are equal between the two datasets. Points represent individual measurements and lines represent predictions of the best fitting model for each replicate at each temperature.

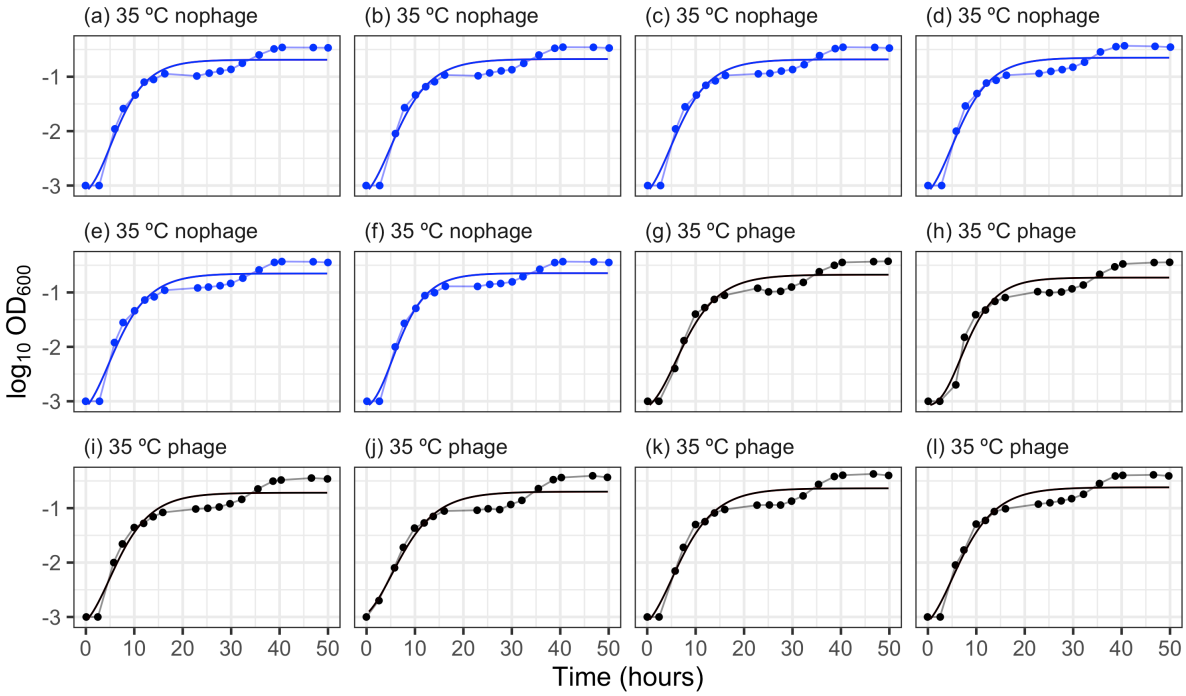

Figure S7. Effect of data cleaning on logistic growth curves for bacterial growth in the presence (black) and absence (blue) of phage at 35 ºC. The Gompertz model for logistic growth was fitted to each independent replicate and the exponential growth parameter was extracted for use in the thermal performance curves. Points that were removed in the final dataset and predictions of the model using the raw dataset are shown in red. A lack of red indicates no points were removed and predictions are equal between the two datasets. Points represent individual measurements and lines represent predictions of the best fitting model for each replicate at each temperature.

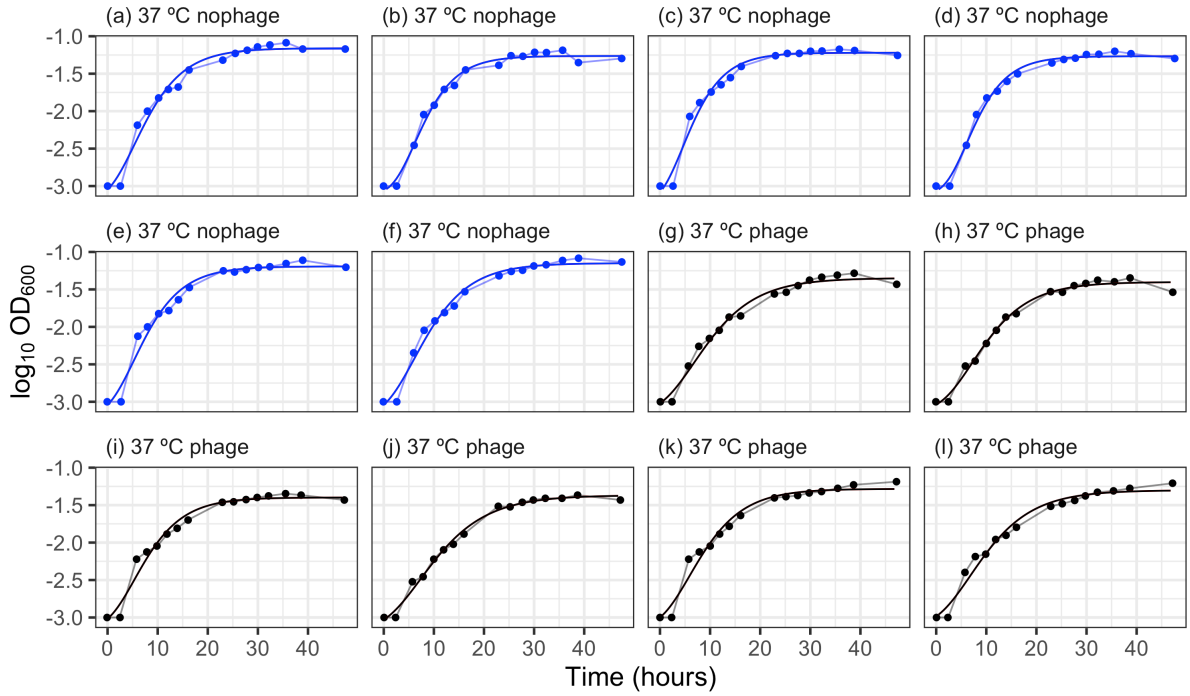

Figure S8. Effect of data cleaning on logistic growth curves for bacterial growth in the presence (black) and absence (blue) of phage at 37 ºC. The Gompertz model for logistic growth was fitted to each independent replicate and the exponential growth parameter was extracted for use in the thermal performance curves. Points that were removed in the final dataset and predictions of the model using the raw dataset are shown in red. A lack of red indicates no points were removed and predictions are equal between the two datasets. Points represent individual measurements and lines represent predictions of the best fitting model for each replicate at each temperature.

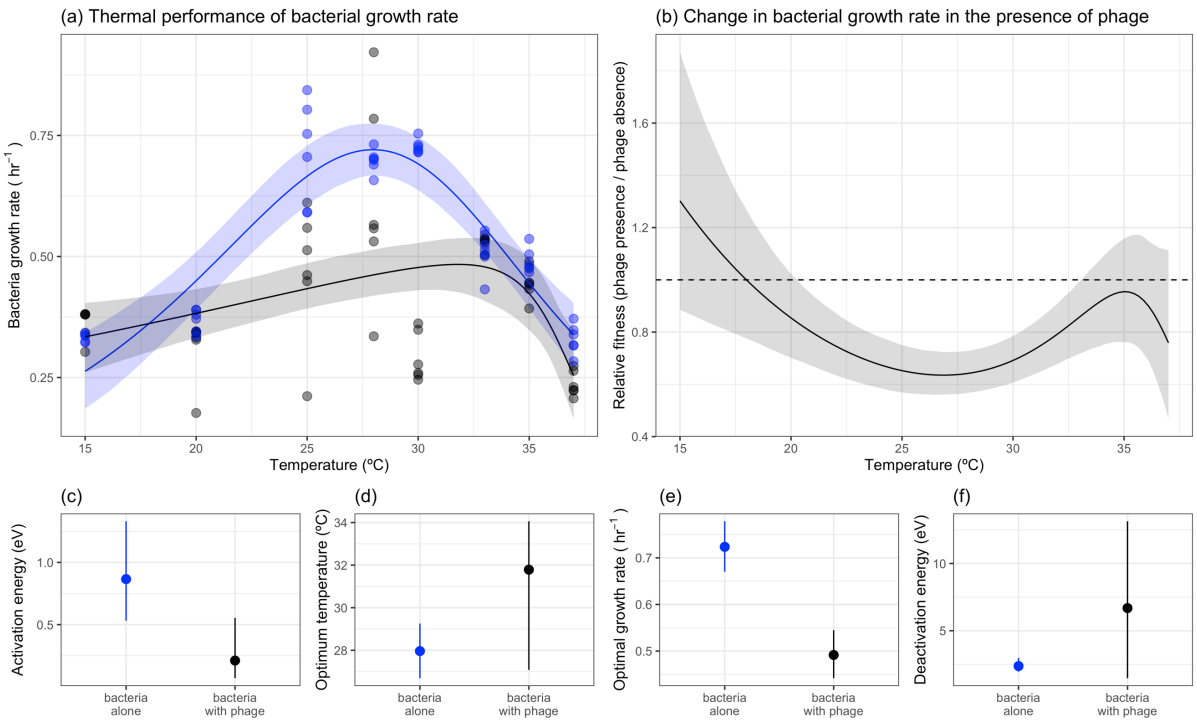

Figure S9. Effect of phage on the thermal performance of bacteria using the raw data. (a) Bacteria growth shows unimodal responses to temperature in the presence (black) and absence of phage (blue). However, phage changed the shape of the thermal response. (b) Phage altered the growth rate of bacteria (calculated as relative fitness) in a non-linear fashion with increasing temperatures. (c-f) The effect of phage on key thermal performance traits. Phage altered the (c) activation energy, (d) optimum temperature, (e) optimal growth rate and (f) deactivation energy. In (a) the solid line represents the mean prediction and shaded band represents the 95% credible interval of predictions. The dashed line at y = 1 would indicate that phage do not alter growth rate. Below 1, phage reduces the growth rate of the bacteria. In (c-f) points and lines represent the mean and 95% credible intervals of the estimated parameters.

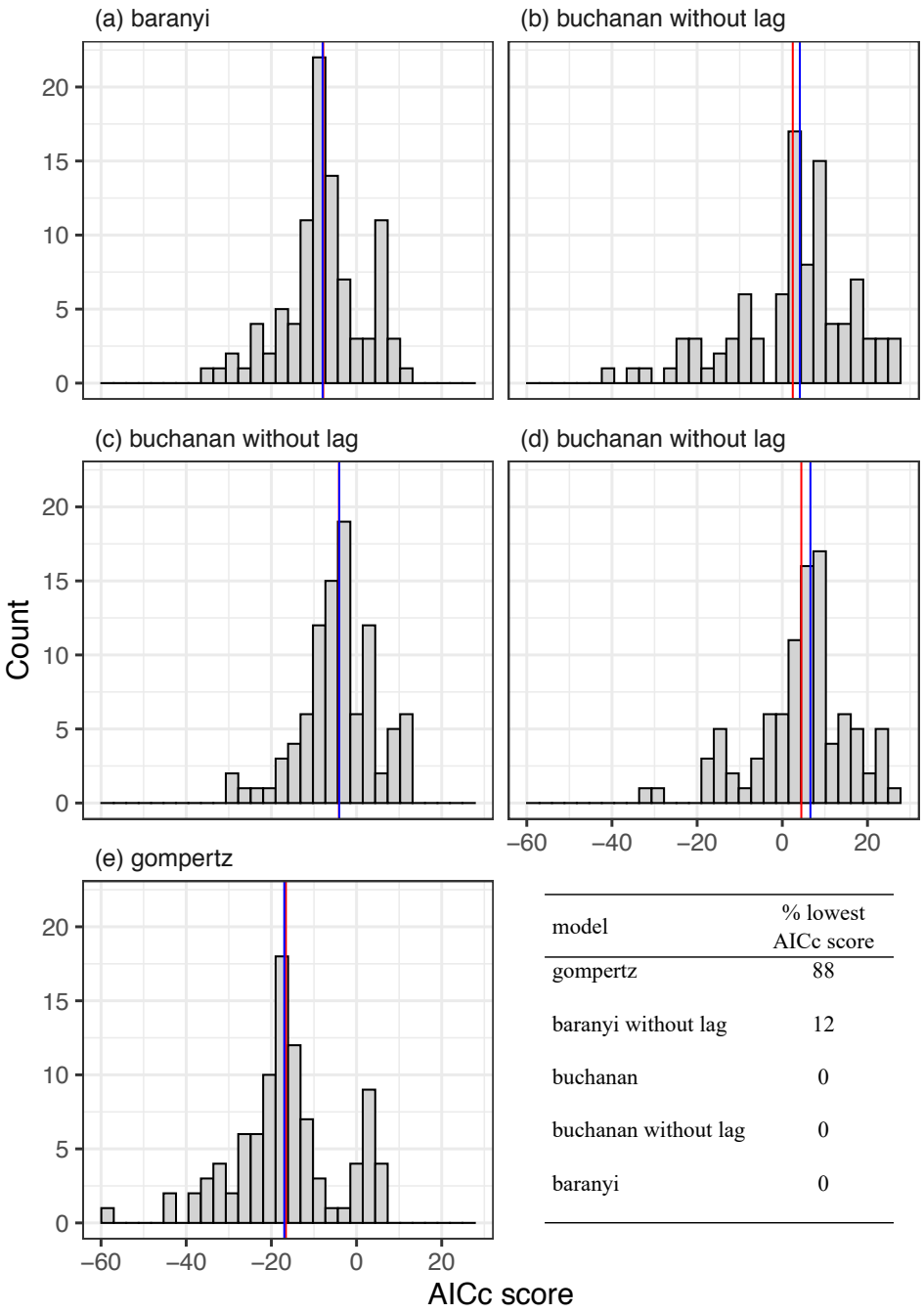

model	% lowest AICc score
gompertz	88
baranyi without lag	12
buchanan	0
buchanan without lag	0
baranyi	0

Figure S10. Distribution of AICc scores for different logistical growth models fitted to bacteria growth in the presence and absence of phage. Numerous logistical growth models were fitted to each bacterial growth curve in the presence and absence of phage. The Akaike's Information Criterion score adjusted for small samples (AICc) for each model was calculated and compared across models to select the best, consensus model. The table in the bottom right demonstrates that for 74% of the curves, the Gompertz model returned the lowest AICc score. The red and blue lines per panel represent the mean and median AICc score of that model respectively.

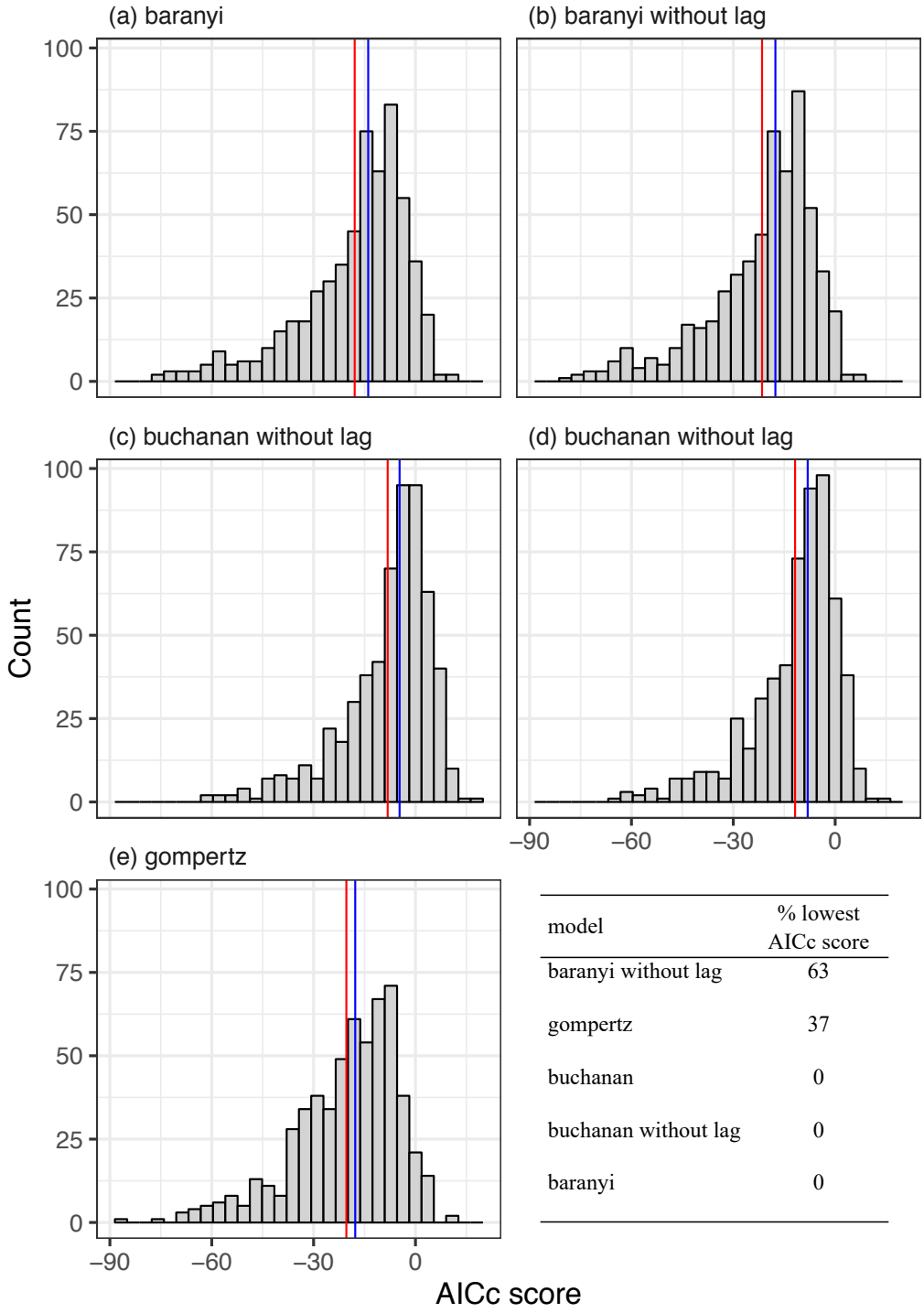

model	% lowest AICc score
baranyi without lag	63
gompertz	37
buchanan	0
buchanan without lag	0
baranyi	0

Figure S11. Distribution of AICc scores for different logistical growth models fitted to bacteria growth of susceptible and resistant clones. Numerous logistical growth models were fitted to each bacterial growth curve in the presence and absence of phage. The Akaike's Information Criterion score adjusted for small samples (AICc) for each model was calculated and compared across models to select the best, consensus model. The table in the bottom right demonstrates that for 63% of the curves, the Baranyi model without a lag phase returned the lowest AICc score. The red and blue lines per panel represent the mean and median AICc score of that model respectively.

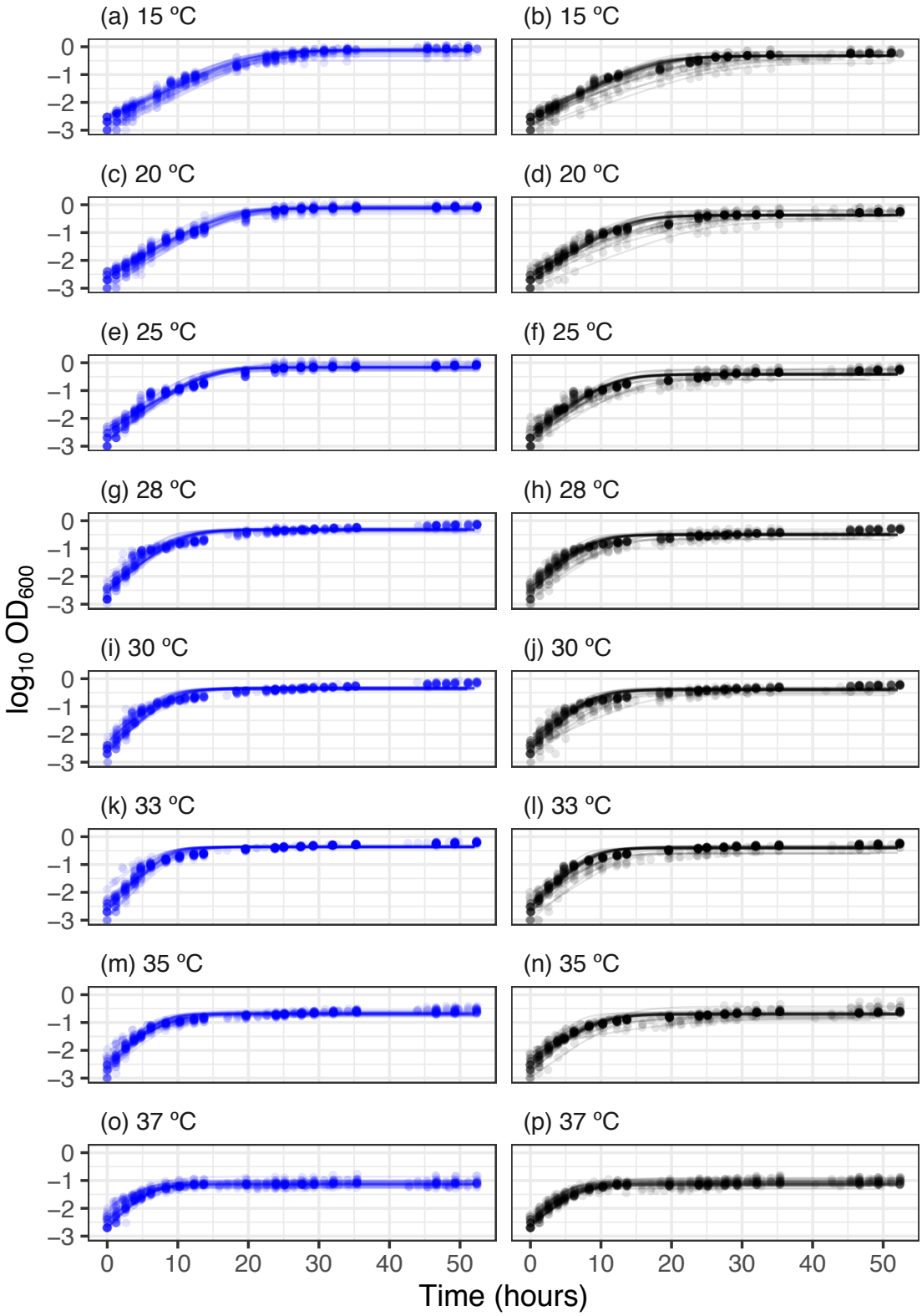

Figure S12. Logistic growth curves for bacterial growth of susceptible (blue) and resistant (black) clones. The Baranyi model without a lag phase was fitted to each independent replicate and the exponential growth parameter was extracted for use in the thermal performance curves. Points represent individual measurements and lines represent predictions of the best fitting model for each replicate at each temperature.

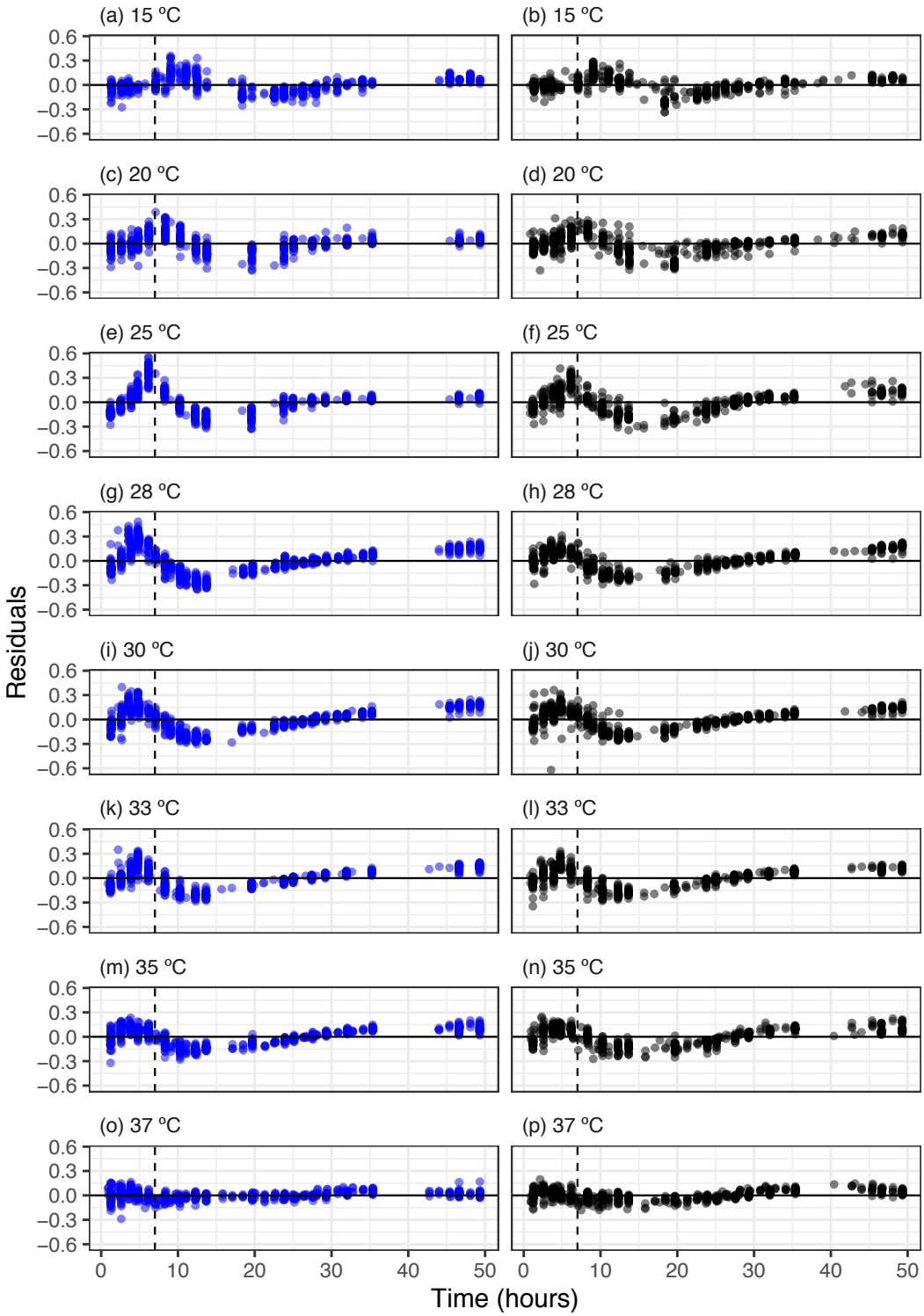

Figure S13. Fit residuals through time of logistic growth curves of susceptible (blue) and resistant (black) bacterial clones. The residuals of the Baranyi model without a lag phase were plotted as a function of time for each clone. There is some systematic variation in the residuals that are similar across most temperatures and resistant and susceptible clones. However, there does appear to be systematic variation in the first 7 hours after growth was first measured which could result in growth being underestimated at some temperatures more than others. The vertical line is drawn after 7 hours after growth was first detected and is a key portion of the curve used to estimate exponential growth rate.

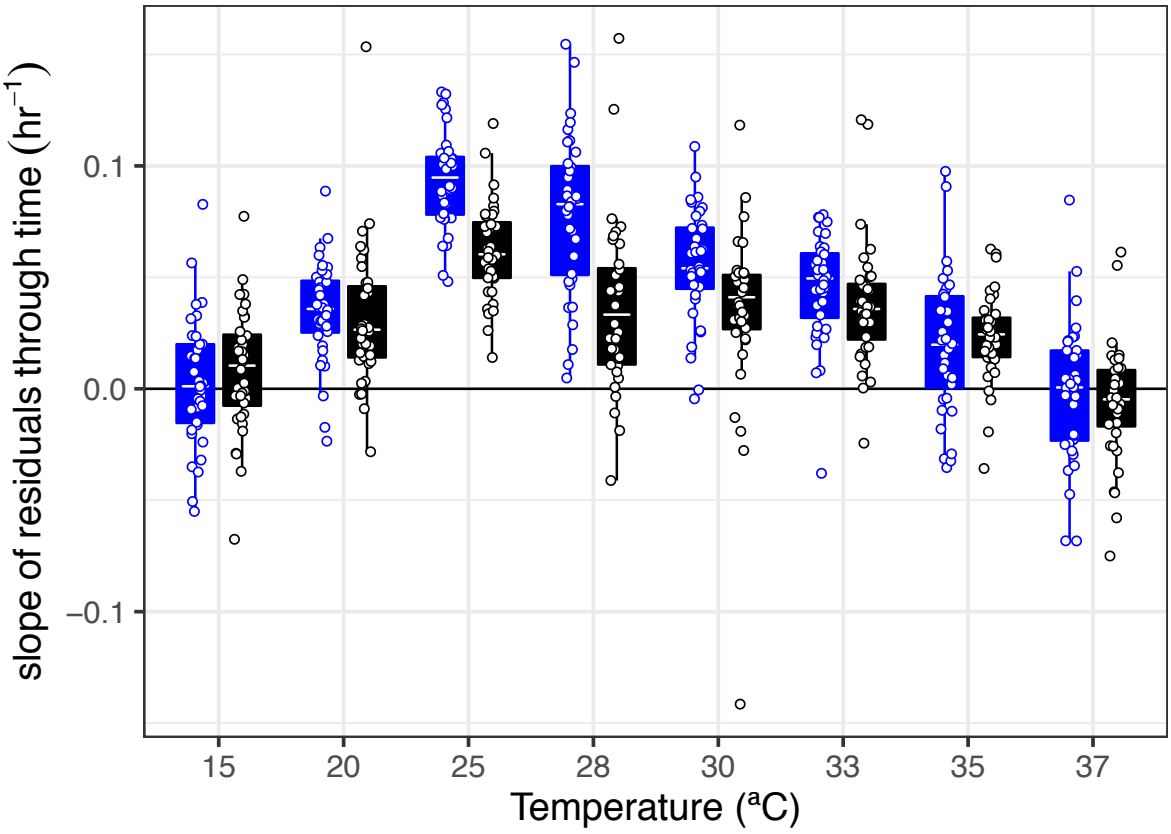

Figure S14. Systematic variation in the residuals during the exponential growth phase of susceptible (blue) and resistant (black) bacterial clones. The slope between the residuals and time over the first 7 hours growth was detected was investigated. A slope of 0 would indicate that the model estimates exponential growth adequately, whereas a slope greater than 1 would indicate that the model underestimates growth rate given the data. Exponential growth rate is underestimated at temperatures where bacteria grew best, and at these temperatures there was a significantly greater underestimation of growth rate in susceptible, rather than resistant bacteria. Points represent the slope of individual fits. Tops and bottoms of the bars represent the 75th and 25th percentiles of the data, the white lines are the medians, and the whiskers extend from their respective hinge to the smallest or largest value no further than 1.5 * interquartile range.

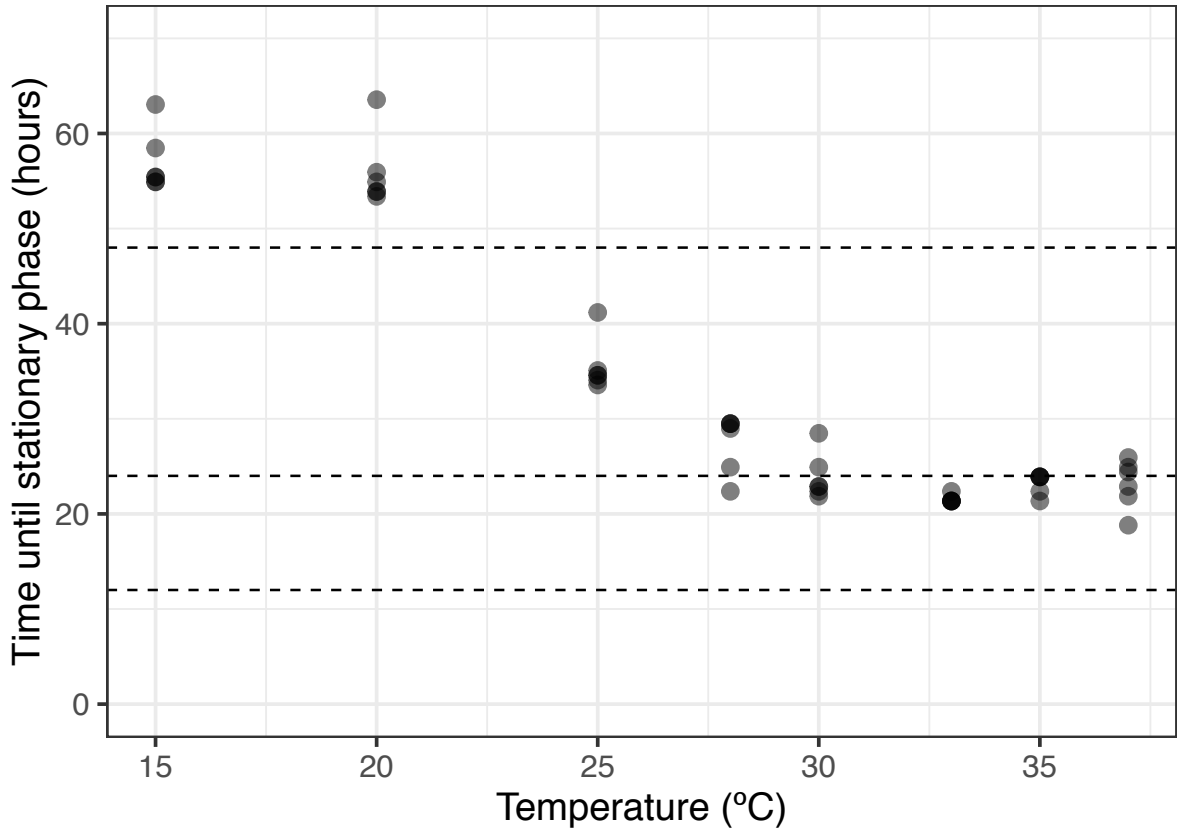

Figure S15. Time to stationary phase of bacteria growth in the presence of phage across temperatures. Time to stationary phase was estimated as the time at which the predictions of the model were 90% of the estimated carrying capacity, $log_{10}n_{max}$. Temperatures above 20 ºC are all in stationary phase before the final sampling point of 48 hours, indicating nutrient limitation between 24 and 48 hours at these temperatures. Points represent the time to stationary phase of independent replicates. Dashed lines indicate the times at which samples were taken to test for resistance in equivalent trials.

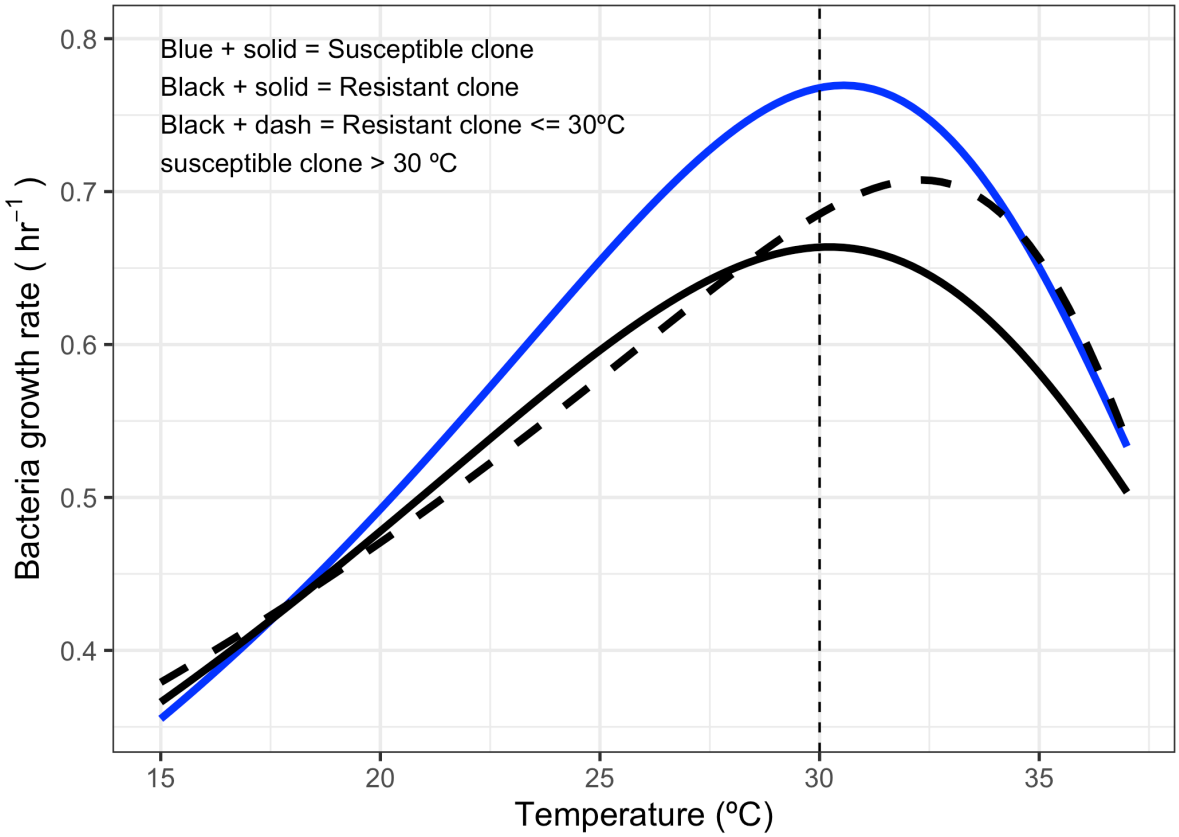

Figure S16. Temperature dependent evolution and cost of resistance in *Pseudomonas fluorescens*. The thermal performance of the average susceptible clone (blue, solid line) and resistant clone (blue, solid line) represent the same curve as in Figure 4. However, there is very little phage infection beyond 30 ºC (Figure 3), so to emphasise the effect of ecological (differences in CT_{max}) and evolutionary (evolution of resistance) mechanisms, we plotted the modelled thermal performance curve of the average resistant clone at temperatures <= 30 ºC and the average susceptible clone at temperatures > 30 ºC. The shift in T_{opt} observed in Figure 1 is only visible by combining ecology and evolutionary mechanisms. Lines represent predictions based on the model fit to the mean rate values for each curve in (Figure 4). Dashed, vertical line represents the CT_{max} of the phage, beyond which little phage infection occurred.